The Ocular Surface 29 (2023) 314–330

Contents lists available at ScienceDirect

The Ocular Surface

journal homepage: www.elsevier.com/locate/jtos

New trends towards glaucoma treatment: Topical osmoprotective microemulsions loaded with latanoprost

J.J. López-Cano [a,b], M.A. González-Cela-Casamayor [a,b], V. Andrés-Guerrero [a,b], M. Vicario -de-la-Torre [a,b], J.M. Benítez-del-Castillo [b,c], R. Herrero-Vanrell [a,b,*], I.T. Molina-Martínez [a,b,**]

[a] Innovation, Therapy and Pharmaceutical Development in Ophthalmology (InnOftal) Research Group, UCM 920415, Department of Pharmaceutics and Food Technology, School of Pharmacy (UCM), Plaza Ramón y Cajal s/n, Madrid, 28040, Spain
[b] Ocular Pathology National Net (OFTARED) of the Institute of Health Carlos III, Health Research Institute of the San Carlos Clinical Hospital (IdISSC), Madrid, 28040, Spain
[c] Ocular Surface and Inflammation Unit, Ophthalmology Department, Sanitary Research Institute of the San Carlos Clinical Hospital (IdISSC), Madrid, 28040, Spain

ARTICLE INFO

Keywords:
Osmoprotection
Microemulsion
Latanoprost
Osmoprotective microemulsion
Glaucoma
Cell internalization

ABSTRACT

The chronic use of hypotensive agents eventually leads to ocular surface damage and poor patient compliance during glaucoma management. Thus, new sustained drug delivery systems are needed. This work aimed to develop osmoprotective latanoprost-loaded microemulsion formulations as new potential glaucoma treatments with ocular surface protective properties. The microemulsions were characterized and latanoprost encapsulation efficacy determined. *In-vitro* tolerance, osmoprotective efficacy, cell internalization as well as cell-microemulsion interactions and distribution were performed. *In vivo* hypotensive activity was conducted in rabbits to assess intraocular pressure reduction and relative ocular bioavailability. Physicochemical characterization showed nanodroplet sizes within 20–30 nm, being *in vitro* tolerance within 80 and 100% viability in corneal and conjunctival cells. Besides, microemulsions exhibited higher protection under hypertonic conditions than untreated cells. Cell fluorescence lasted for 11 days after short exposure to coumarin-loaded microemulsions (5 min) showing extensive internalization in different cell compartments by electronic microscopy. *In vivo* studies exhibited that a single instillation of latanoprost-loaded microemulsions reduced the intraocular pressure for several days (4–6 days without polymer and 9–13 days with polymers). Relative ocular bioavailability was 4.5 and 19 times higher than the marketed formulation. These findings suggest the use of these microemulsions as potential combined strategies for extended surface protection and glaucoma treatment.

1. Introduction

Among all the different causes of vision loss in the world, there are some chronic ophthalmic diseases that are inherently more difficult to treat than others such as it is the case of age-related macular degeneration, diabetic retinopathy, glaucoma, and genetic diseases related with retinal degeneration. That is one of the main reasons why the world health organization (WHO) created the "Vision 2020: The Right to Sight" program in order to achieve a reduction of preventable vision loss diseases by 2020 [1]. Glaucoma is considered a group of eye diseases that causes irreversible blindness in the world being the intraocular pressure, the main risk factor. When prolonged periods of chronic hypertension occurs, glaucoma patients eventually experiment optic nerve degeneration and ultimately, vision loss [2]. One of the first line therapeutic strategies to tackle glaucoma progression is the topical administration of hypotensive agents. There are different pharmacological groups of topical hypotensive therapies for the management of glaucoma, such as beta-blockers, carbonic anhydrase inhibitors, α-adrenergic agonists, prostamides or prostaglandin analogs. In many cases, a combination of hypotensive drugs is needed to successfully control intraocular pressure (IOP). Among all different therapies, topical

* Corresponding author. Innovation, Therapy and Pharmaceutical Development in Ophthalmology (InnOftal) Research Group, UCM 920415, Department of Pharmaceutics and Food Technology, School of Pharmacy (UCM), Plaza Ramón y Cajal s/n, Madrid, 28040, Spain.
** Corresponding author. Ocular Pathology National Net (OFTARED) of the Institute of Health Carlos III, Health Research Institute of the San Carlos Clinical Hospital (IdISSC), Madrid, 28040, Spain.
E-mail addresses: rociohv@ucm.es (R. Herrero-Vanrell), iremm@ucm.es (I.T. Molina-Martínez).

https://doi.org/10.1016/j.jtos.2023.05.013
Received 9 March 2023; Received in revised form 29 May 2023; Accepted 30 May 2023
Available online 8 June 2023

Nomenclature

DED	Dry Eye Disease
BM	Blank microemulsion
OA	Oleanolic acid
CLU	Clusterin
HA	Hyaluronic acid
ΔIOP	IOP pressure reduction
ΔIOPmax	Maximum percentage of ΔIOP
tonset	onset time
teffective	effective time
$AUC_{0-t'}$	Area under the ΔIOP (%) time curve from 0 to effective

prostaglandins have been studied for being highly more effective than other antiglaucomatous agents in lowering IOP in certain periods of treatment (>3 months) [3]. Particularly, latanoprost is considered one of the most effective hypotensive drugs achieving good effectivity for 24-h periods [4].

Despite their advantages in lowering IOP, many glaucoma drugs are related to local and systemic side effects such as high risk of low heart rate, hyperaemia (beta-blockers), altered taste, blurred vision (alpha agonists and anhydrase inhibitors) and eye lid changes or darkening as well as irritation (prostaglandins) [5]. Furthermore, patients exposed to chronic treatments with topical hypotensive drugs might present signs and symptoms of dry eye disease. These correlation between glaucoma treatment and dry eye are frequently due to a destabilization of the precorneal tear film being the main responsible, the components of the ophthalmic formulations (frequently preservatives) or even the hypotensive substances. To all these, it must be added the low bioavailability of topical formulations due to their fast elimination from the ocular surface (less than 5% of the administered drug, is able to permeate the different barriers and reach intraocular tissues) [6]. Therefore, enhancing permeation and increasing residence time of hypotensive drugs is a critical factor to bear in mind when developing future therapies for glaucoma treatment.

In summary, there are several critical factors that need to be considered when selecting the appropriate treatment for glaucoma such as patient compliance, effectiveness or absence of adverse effects [7]. It is evident that the development of novel ophthalmic formulations based on drug delivery systems able to avoid successive applications and at the same time protecting the ocular surface is a challenge in the treatment of glaucoma.

Drug delivery systems overcoming corneal barriers for the treatment of glaucoma and able to enhance ocular drug delivery of hypotensive agents are under study. Among them, pharmaceutical nanosystems are of great interest. Polymeric nanoparticle suspensions made of different biomaterials have been studied for enhancing corneal drug delivery. In the group of nanoparticulate systems, biodegradable polymers (PLGA, PLA), natural polymers (chitosan, gelatin, sodium alginate) or proteins (albumins) have successfully demonstrated their ability to surpass ocular barriers [8]. Liposomes have been widely a studied as drug delivery systems for ocular surface applications since their intrinsic properties such as low surface tension, lipidic nature and bilayer membranes make them suitable for restoring ocular surface tear film while increasing drug permeation through corneal structures [9]. Besides, the possibility to modify their structure and provide them with specific charges offer attractive possibilities [10]. Alike liposomes, niosomes are lipidic structures with double bilayers but made up of non-ionic surfactants. Their advantages over liposomes are their chemical stability, less immunogenicity and better fluidity. Niosomes have demonstrated both high efficacy and encapsulation efficiency [8] and in particular encapsulating hypotensive drugs [11]. Dendrimers are substances chemically synthesized forming branch-like structures. They can be sized and functionalized to interact with certain cellular domains [12]. Moreover, they can be combined with mucoadhesive polymers and provided with high solubilization ratios, however they might cause blurry vision or discomfort [8]. Cyclodextrins are able to create inclusion complexes entrapping hypotensive drugs presenting different properties. These oligosaccharides can act as depot systems in some cases, increase topical bioavailability and also improve tolerability [13]. Microemulsions and nanoemulsions have gained a lot of interest over the last few years as topical therapies for the treatment of ocular pathologies, mainly dry eye disease, since they combine both aqueous and lipid-base components [14]. Besides, as both pharmaceutical systems include surfactants the permeation and delivery of lipophilic substances could be facilitated [15]. The term microemulsion is used to described thermodynamically stable systems with very small sizes (often less than 100 nm) that can be prepared with low energy methods with spheric or non-spheric structures depending on the surfactant optimum curvature. Nanoemulsions comprises usually higher sizes than microemulsions (100–500 nm) although less than 100 nm could also be present. They are often developed by high energy methods such as high homogenization and resulted always sphere-shaped [16]. Ikervis® is an example of a marketed cationic cyclosporin nanoemulsion for the treatment of DED [17]. This novel therapy has been developed through the Novasorb technology, based on the preservative-free nanoemulsion system (Cationorm®) initially developed as an artificial tear formulation [18].

Among the most relevant characteristics of microemulsions is the stability of the nanodroplet sizes that remain almost unaltered over time unless chemical or microbiological degradation of their components occurs. These mentioned properties make them ideal to achieve high retention of lipophilic drugs. Furthermore, they required low energy for the fabrication procedure facilitating their scalability [19]. Attending to their composition, microemulsions requires several components such as an oily phase, surfactant, cosurfactant, an aqueous phase and also may include co-solvents. Since several years ago, microemulsions are acquiring a lot of attention in the treatment of dry eye disease because they provide lipid and aqueous substances that help preocular tear film restoration [20]. These micellar systems own low surface tension, enhancing their extensibility on the ocular surface after instillation [21]. Furthermore, microemulsions have also been studied for their ability to increase drug bioavailability and retention time more than other pharmaceutical systems [21].

Therefore, their compatibility with the ocular surface and precorneal tear film, together with their high retention time and permeability make microemulsions suitable systems for the incorporation of hypotensive drugs as anti-glaucoma treatment. Beside hypotensive drugs, some specific actives such as amino acids, sugars, proteins, re-epithelizing substances or polymers can be included in topical ophthalmic microemulsions to provide hypotensive activity with and additional antioxidant, anti-inflammatory or osmoprotective properties able to protect the ocular surface [22]. Recently, the addition of actives with different protective properties have gain special interest to help the homeostasis of the damaged ocular surface [23].

Among the substances with potential protective activity on the ocular surface are amino acids as betaine, L-carnitine, leucin, proline and glycine. The first two ones are able to regulate cellular volume, decrease inflammation, increase anti-oxidation or decrease cell death linked to hypertonic stress on the ocular surface caused by tear film destabilization [24]. Leucin with anti-inflammatory properties on the ocular surface along with proline or glycine, all responsible of collagen fibrils formation [22]. Clusterin (CLU) is a promising agent described for the treatment of DED and ocular surface diseases promoting the sealing of disrupted corneal barrier. CLU possess antiapoptotic activity with the capability to counteract barrier disruption events produced by inflammation and desiccating stress both present in DED [25]. Another enticing substance is oleanolic acid (OA), a lipidic pentacyclic triterpene able to inhibit matrix metalloproteinase (MMP) activity promoting cell survival of corneal cells. OA has also been reported for inhibiting nitric

oxide synthase (NOS) activity, thus decreasing inflammation and oxidative stress [26]. Squalene is a potent antioxidant with potential protective properties for the ocular surface, such as anti-inflammatory or ROS scavenger [27]. Also, mucoadhesive polymers such as hyaluronic acid (HA) or hydroxypropylmethylcellulose (HPMC) have been widely employed for the treatment of mild to moderate ocular surface diseases. On the one hand, HA have previously shown anti-inflammatory properties [28] in the ocular surface on human trials [29] and anti-apoptotic activity in *in vitro* cell culture models of hyperosmolarity [30]. On the other hand, HPMC is commonly employed in artificial tears increasing retention time and protective properties on the ocular surface (anti-inflammatory, antiapoptotic and cell volume regulator) [30,31].

In this study we aimed to develop a long-acting topical ophthalmic microemulsions containing the prostaglandin latanoprost and osmoprotective and mucoadhesive substances with ocular surface protecting activity and high residence time. For this purpose, we previously developed and optimized a topical osmoprotective microemulsion for ocular surface protection based on Betaine, Leucin, Clusterin and Oleanolic acid osmoprotectants [32]. With the inclusion of latanoprost to this formulation, the aim was to create a new generation of hypotensive glaucoma therapies with increased activity as well as promoting ocular surface protection and eliminating the drawbacks associated to glaucoma therapies.

2. Methods and materials

2.1. Materials

Propylene glycol, squalene (≥98%), soybean oil (unsaturated triglycerides), Kolliphor EL® and ethyl oleate, and Leucine were purchased from Merck (Madrid, Spain). Lipoid soy phosphatidylcholine (PC) (Phospholipon 90G®) was acquired from Lipoid GmbH (Ludwigshafen, Germany). Betaine (98%), Trehalose dihydrate, Dextran clinical grade 60–80 KDa and oleanolic acid (OA) (97%) were purchased from Fisher Scientific (Madrid, Spain). Human recombinant clusterin (CLU) was purchased from Biogen científica (Madrid, Spain). Latanoprost (Lt) was purchased from MedChem Express (Sollentuna, Sweden). MTT, glutaraldehyde solution 50 wt % and osmium tetroxide 99.8%, paraformaldehyde DAC 95–100.5% (PFA) were also purchased from Merck (Madrid, Spain). Hyaluronic acid (HA), MMW (400–800 KDa) was purchased from Abarán materias primas (Madrid, Spain).

2.2. Hypotensive microemulsions development

An O/W microemulsion was developed by self-emulsification as previously developed by our group [32]. The microemulsion is composed of 0.8% ethyl oleate, 0.2% squalene and 0.2% of soybean oil as the oily phase. Besides, 1% propylene glycol as well as 0.5% soy phosphatidylcholine (PC) and Kolliphor EL® were included as cosolvent and surfactants respectively. In this sense in order to create the hypotensive microemulsion, latanoprost was dispersed in ethyl oleate in a concentration of 50 μg/μL. Then 10 μL of ethyl oleate (0.085%) containing latanoprost (500 μg) were taken and added to the rest of the oily phase (0.715% ethyl oleate, 0.2% squalene, 0.2% of soybean oil and 1% of Kolliphor EL®). The rest of the components were added as described above. The oily phase, cosolvents and surfactants were mixed and dissolved (400 rpm and 25 °C) in a 10 mL glass vial until a transparent oily solution was formed. Furthermore, the formulation was made isotonic by adjusting the amount of included di-hydrated trehalose and osmoprotective susbtances. After that, the aqueous phase was added in a single step over the oil phase under agitation (1000 rpm). Finally, microemulsions were kept overnight at 2-8 °C for maturation. The osmoprotective hypotensive microemulsions were made as follows: betaine (0.4%) and leucin (0.9%) were combined for the development of formulation A-Lt and adding HA (0.2%) to create formulation A-HA-Lt. Moreover, the combination of OA (0.01%) and CLU (50 μg/mL) was made in order to create B-Lt formulation, adding dextran (0.1%) for formulation B-DXT-Lt. All the osmoprotective susbtances were included in the aqueous phase except for the OA that was included in the oil phase.

2.3. Physicochemical characterization of microemulsions

2.3.1. Particle size determination

Microtrac® S3500 Series Particle Size Analyzer (Montgomeryville, PA, USA) was employed for DLS (dynamic light scattering) analysis. The samples were diluted in ultrapure water (1:2) following the manufacturer's procedure.

2.3.2. SEM and Cryo-TEM experiments

Cryo-EM; 200 kV FEI TALOS Arctica was employed to evaluate the morphology of the developed nanosystems. Besides, SEM; JEOL JSM 7600F was used to assess the surface and 3D structure of the microemulsion's nanodroplets. Cryo-EM was performed by placing 3 μL of microemulsions onto Lacey Carbon film Cu/Rh lacey carbon grids, blotted, using a FEI Vitrobot Mark IV to plunge them into liquid ethane. Furthermore, a Talos Arctica was employed to analyze the microemulsions by using a X field emission gun operating at 200 kV. EPU Software (ThermoFisher Scientific ®) on a Falcon III was used to acquire the images. They were recorder under low-dose conditions at a nominal magnification of 73000 (1.4 Å/pixel sampling rate respectively). Finally, ImageJ (Fiji) analysis software 2.1.0/1.53c (National Institute of Mental Health, Bethesda, Md USA) was used to analysis the images. Microemulsions were fixed in Whatman® Nuclepore™ polycarbonate membranes (25 mm diameter, 0.1 μm pore size) by staining and fixation with green malachite according to previous studies [33] with some modifications based on our developed nanosystems. After that, the polycarbonate membranes were submerged for 10 min in each sample. Furthermore, samples were stained for 1 h at 4 °C in a malachite (1%) - glutaraldehyde (3%) solution prepared in phosphate-buffered saline (PBS). Finally, polycarbonate membranes containing the samples were posteriorly fixated for 1 h with osmium tetroxide (1%) at room temperature. Following that, serial dehydration with ethanol (30%, 50%, 70%, 90% and three times 100%) was performed and samples were freeze dried overnight. For SEM visualization, fixated samples in the above-mentioned membranes were placed in a conductive carbon adhesive tape and adhered to SEM disks. SEM disks were coated with chromium oxide (8 nm) (Leica EM ACE600) and visualized in a JEOL JSM 7600F. The magnification employed was 50000 at 15 kV.

2.3.3. Zeta potential

Autosizer 4700, Malvern was employed for zeta potential analysis of the different nanodroplets of the microemulsions. The analysis was carried out at room temperature by using folded capillary zeta cells.

2.3.4. pH

The developed hypotensive microemulsions were measured with a pH-meter (model 230, Mettler, Barcelona, Spain) equipped with a microelectrode (InLab, Mettler, Madrid, Spain). The pH-meter was properly calibrated with different pH solutions (pH 9 and pH 4 respectively) weekly.

2.3.5. Surface tension

A force tensiometer (K-11, Kruss) equipped with Wilhelmy plate was used to determine the mean average surface tension of the microemulsions developed in the present article. As a calibration step, MilliQ water was analyzed (72.0 ± 1.5 mN/m) before sample measurements. The tensiometer was preset at 33 °C and warmed for 3 min before microemulsion analysis.

2.3.6. Rheological studies

A Discovery HR1 hybrid Rheometer – TA instruments (New Castle,

DE, USA) equipped with a 60 mm diameter parallel plate system adjusted to 0.6 mm gap. The conditions employed for the analysis included shear rates from 0 to 1000 s^{-1} in 30 steps at room temperature.

2.3.7. Osmolarity

The osmolarity of formulations was measured by a freezing point depression osmometer Fiske micro-osmometer, model 210 (Tecil, Madrid, Spain) calibrated with 50, 290 and 850 mOsm/L calibration standards.

2.4. HPLC determination

An isocratic method was employed for the quantification of latanoprost by HPLC. The analysis was carried out using RP-HPLC in an Acquity Arc Bio® (Waters, Madrid, Spain) UHPLC equipped with a photodiode array detector (2998 PDA Detector), a bioSample Manager FTN-R and a bioQuaternary Solvent manager-R. For the separation, an Ascentis® C18 (25 cm × 4.6 mm; 5 μm) column was employed. The mobile phase was comprised of acetonitrile and water acidified with TFA 0.1% (60:40) HPLC grade based on a pre-existing method [34]. A flow rate of 1 mL/min and a wavelength of 210 nm were used. The column temperature was set at 30 °C and the sample injection volume was 10 μL. Different standard concentrations were prepared to elaborate the calibration curve. The range of the concentrations used was 200, 100, 50, 25, 10 and 5 μg/mL prepared in absolute ethanol from a 1 mg/mL stock solution in ethanol. Limit of detection (Y-intercept divided by slope) and quantification (3.3 times the limit of detection) were also calculated to determine the maximum range of quantification when no sample is detected.

2.5. Encapsulation efficiency

For the quantification of the total amount of latanoprost present in the formulations, the microemulsions (A-Lt, A-HA-Lt, B-Lt, and B-DXT-Lt) were freeze dried overnight, incubated in ethanol absolute 10 min, spin, passed through 0.22 μm nylon filter and injected to the chromatographic system. Total yield was calculated by dividing concentration of latanoprost present in each sample by the theoretical concentration (50 μg/mL). To determine the residual latanoprost present in the aqueous phase and calculate the entrapped latanoprost, an ultrafiltration method was used. To this, 0.5 mL of each sample was introduced in Amicon® Ultra - 0.5 mL tubes comprised of Ultracel® - 50 KDa centrifugal filters. Afterwards, samples were centrifuged at 14.000 rpm for 15 min in a Mikro 220R centrifuge (Hettich, Tuttlingen, Germany). Briefly, the filtered aqueous phases were freeze dried overnight, redissolved in 1 mL of ethanol absolute (solubilization of residual latanoprost) and spined for 3 min. Finally, samples were spined and filtered through 0.22 μm nylon filters to remove any remanent trehalose or water-soluble substances (insoluble in ethanol) and injected into the chromatographic system (10 μL). To calculate the encapsulation efficiency (EE), total amount of detected latanoprost was subtracted to the drug present in the aqueous filtrate and divided by the total amount times % (Equation (1)).

$$EE\,(\%) = \frac{Total\ amount\ of\ latanoprost - latanoprost\ in\ aqueous\ filtrate}{Total\ amount\ of\ latanoprost}\ x\,100 \quad (1)$$

2.6. Cell culture studies

2.6.1. Human conjunctival and corneal epithelial cells

Human immortalized conjunctival epithelial cells (HConEpiCs, Innoprot, Bizkaia, Spain) and human immortalized corneal epithelial cells (HCECs; Evercyte GmbH, Vienna, Austria) were used for the different experiments carried out. Besides HCECs were employed for osmoprotective efficacy determination. The cells were kept under controlled conditions (37 °C, 5% CO_2 and 95% humidity) and cell culture media was changed every 48 h. HConEpiCs was cultured in IM-Ocular Epithelial Cell Medium (Innoprot, Bizkaia, Spain) and the cells culture in collagen I coated flasks at 5 μg/cm^2 (Innoprot, Bizkaia, Spain). Furthermore, HCECs were maintained in EpiLife® cell culture media (Life Technologies, Madrid, Spain) supplemented with penicillin-streptomycin 1% and EDGS® 1X (Life Technologies, Madrid, Spain).

2.6.2. Viability in human corneal and conjunctival epithelial cells

HConEpiCs and HCECs were used for the *in vitro* tolerance studies. Cells were exposed to osmoprotective microemulsions including latanoprost for 1 h and 4h. HConEpiCs and HCECs were seeded in 96 well plates at 30.000 and 20.000 cells/well respectively and incubated overnight. Briefly, supernatants were discarded, and cells exposed to the different selected times. Following that, Dulbecco's phosphate-buffered saline (DPBS) was added to the wells twice to wash any remaining formulation. Furthermore, a final MTT working concentration of 0.33 mg/mL was obtained by mixing cell culture media and MTT stock solution (1:6). MTT working solution was added to the wells and incubated for 4 h. Finally, supernatants were discarded and 100 μL of DMSO added to each well to dissolve formazan crystals. The plates were shaken for 5 min and measured in the spectrophotometer (550 nm). In all toxicity assays benzalkonium chloride (0.005%) was used as positive control [31].

2.6.3. Osmoprotection studies in an in vitro hyperosmolar model of human corneal epithelial cells

The different hypotensive formulations (A-Lt, A-HA-Lt, B-Lt and B-DXT-Lt) with osmoprotective properties were evaluated in a hyperosmolar stress model developed and optimized previously by our group [30]. For the osmoprotection assessment, 20.000 cells/well were seeded in 96 well plates and incubated overnight. Following that, supernatants were removed and the microemulsions and isotonic sodium chloride for the controls (used for positive and negative control) were added to each well following a 2-h incubation. After that, supernatants were again removed, and the wells washed twice with DPBS. Then, a hyperosmolar environment was created by the addition of a hypertonic mixture of NaCl and cell medium (470 mOsm/L) in all wells (except for the negative control) and incubated for 16 h at 37 °C and 5% CO_2. The positive controls were the cells initially in contact to an isotonic sodium chloride (NaCl 0.9%) and then exposed to the hyperosmolar environment. Finally, all the supernatants were discarded, and cell viability measured by MTT addition as previously described.

2.6.4. Internalization studies

2.6.4.1. Fluorescence microscopy. In order to assess the ability of microemulsion internalization, three non-loaded formulations named as base microemulsion (BM), BM with hyaluronic acid (BM-HA) and BM with dextran (BM-DXT) containing coumarin (2 μg/mL) as model fluorescence lipophilic substance were incubated with HCECs and washed twice with DPBS. A coumarin suspension at the same concentration was used to confirm minimum cell fluorescence. The cells were exposed to the different treatments for 5 min to simulate physiological retention time of topical ophthalmic administered treatments (1–10 min) [35,36]. Briefly, 5 × 10^5 cells/well were seeded in 6-well plates and incubated overnight. The supernatants were discarded and 100 μL of each formulation, sodium chloride (negative control) or coumarin suspension (fluorescence control) were added to previously added 900 μL of cell culture medium for 5 min. After that, the cells were washed twice with DPBS, and each well was renewed with fresh media. Finally, HCECs were visualized under a Nikon Eclipse TS100 Inverted phase Microscope equipped with an epi-illumination module using FITC and TRITC filters (Izasa Scientific, Madrid, Spain). Cells were examined under the blue laser (535/617) at 20X magnification and pictures were taken for

different time periods (0, 2, 4, 7, 9 and 11 days) until fluorescence was no longer present. Fiji (Image J) was employed to analyze fluorescence intensity from the images. Corrected total cell fluorescence (CTCF) was assessed to minimize background effect (Equation (2)). Integrated fluorescence density is subtracted to the product of the cell fluorescence mean area and the background fluorescence.

$$\mathrm{CTCF} = \textit{Integrated density} - (\textit{mean area of cells x mean background fluorescence}) \quad (2)$$

2.6.4.2. Flow cytometry. Flow cytometry was also performed to quantify the level of cell fluorescence during the different exposure times until basal values were obtained. Similarly, to the microscopy experiments, 5×10^5 cells/well were seeded in 6-well plates, incubated, and exposed for 5 min to microemulsions. After each incubation time, cells were detached by adding trypsin-EDTA 0.05% for 3 min. Besides, cells were centrifuged at 850×*g* for 10 min, re suspended in DPBS and taken to the flow cytometry core facility. A FC 500 (2-laser, 5-color analysis) flow cytometer equipped with FC 500 CXP software (Beckman Coulter, Madrid, Spain) was employed. Before data analysis and gathering, the system was allowed to warm up for at least 15 min. The flow rate was established at a medium flow rate and each sample recorded data from 100000 events. In order to detect the coumarin signal, the blue/red laser (535/617) was used. Moreover, after SSC/FSC gating, and histogram showing count vs coumarin signal was employed. Besides, fluorescence signal of the negative control was adjusted to 10^0 in the X-axis.

2.6.5. Cell-microemulsion interaction studies by electronic microscopy

Interactions between the latanoprost microemulsions (A-Lt, A-HA-Lt, B-Lt and B-DXT-Lt) and HCECs were studied by SEM and TEM. Different parameters were observed and studied such as cell morphology, adhesion of microemulsions to cell structures, permeation capacity as well as distribution across the surface and inside cellular structures.

For SEM visualization, HCECs were seeded on 13 mm Nunc™ Thermanox™ Coverslips (ThermoFisher, Madrid, Spain) inside 6 well plates at 5×10^5 cells/well and incubated for 24 h. Then, supernatants were discarded, and cells were exposed to 100 μL of different microemulsions or the negative control (NaCl 0.9%) + 900 μL of cell culture during 5 min to simulate retention on the ocular surface as previously reported.

A staining buffer (SB) was previously prepared by mixing 2.26% sodium dihydrogen phosphate (NaH_2PO_4) and 2.52% sodium hydroxide (NaOH) solutions in specific proportions (83:17 ratio respectively) adjusting the final pH to 7.2–7.4 with NaOH. A fixation mixture (FM) (4% paraformaldehyde, 3% glutaraldehyde and 1% green malachite) was made in the SB to ensure both fixation of microemulsions and HCECs. Afterwards, cells were washed twice with DPBS and firstly incubated for 4 h in FM. Then, coverslips were stained in osmium tetroxide (1%) for 1 h at room temperature, incubated overnight in SB and serial-dehydrated with ethanol as above-mentioned and critical point dried (Leica EM CPD 300). Finally, coverslips were mounted in SEM disks and coated with chromium oxide (8 nm) (Leica EM ACE600) as previously mentioned. The magnification employed was ×2000, x15000 and x30000 by using a JEOL JSM 7600F.

JEOL JEM 1400 was used for TEM visualization and the procedure was carried out similarly. HCECs were cultured in 6-well plates (1×10^6/well) and grown for 24 h. Afterwards, supernatants were removed, and cells were exposed to microemulsions as above mentioned for 5 min. Briefly, cells were trypsinized for 3 min and centrifuged (850×*g* for 10 min) in 2 mL centrifuges tubes. Pellets were re suspended in FM and incubated at 4 °C for 6 h. Then, cells were washed twice with SB, centrifuged, and overnight incubated in SB at 4 °C. For the post-fixation procedure, the cells were pelleted and incubated in a 1% osmium tetroxide (OsO_4) and 0.8% potassium ferrocyanide ($C_6FeK_4N_6$) mixture in H_2O for 1 h at 25 °C. Afterwards, cells were washed twice with ultrapure (milliQ) water. Besides, serial-dehydration as previously was performed in ethanol. After dehydration, the samples were embedded in spurr resin (SR) mixed with acetone at different volume ratios for different times (1:3 for 1 h, 1:1 for 1 h and 3:1 for 2 h SR to acetone respectively) and with pure spurr resin overnight at 25 °C. Polymerization of resin was carried out by introducing samples into a 65-70 °C oven for 48 h with tube caps opened. Finally, samples were processed in an ultra-microtome, stained with uranyl acetate, and visualized at 8000x and zoomed 30000x and 150000x.

2.7. In vivo hypotensive effect

Normotensive New Zealand albino rabbits were purchased from Granja San Bernardo (Tarazona, Navarra, Spain) and had an average weigh of 3.39 ± 0.59 kg. Animals were 47 weeks of age, housed in individual cages and feed with a varied diet based on rabbit pellets and vegetables. They were kept ad libitum under controlled conditions of humidity and temperature (50% and 22 °C respectively) with 12/12 h light/dark cycles. Rabbits were gently handled and secured their heads with a surgery towel, ensuring minimal stress and optimal stability for accurate readings. Animals were handled following the ARVO (Association for Research in Vision and Ophthalmology) Statement for the Use of Animals in Ophthalmic Vision Research, the European regulatory system for the use of animals in research as well as the European Communities Council Directive (86/609/EEC) and Spanish Regulation of Experimental Studies with Animals (RD 53/2013, February 1; Ref PROEX 114.4/21, July 16, 2020).

Hypotensive efficacy studies of the developed latanoprost microemulsions (A-Lt, A-HA-Lt, B-Lt, B-DXT-Lt), and marketed formulation with a 50 μg/mL latanoprost (Monoprost®) was assessed in 5 rabbits (n = 10 eyes). Non loaded microemulsions (BM, BM-HA, BM-DXT) were also studied. Briefly, 25 μL of each hypotensive formulation were instilled in both eyes of each rabbit. To determine basal IOPs (100%) (Fig. 1), two different measurements were made before instillation (30 min before and just prior to administration). After instillation, IOPs were recorded every hour for 11 h during the first day, 3 times a day the next day and twice daily until the end of the study using an Icare® Tonovet tonometer (Tiolat, Helsinki, Finland). A minimum wash period of 10 days was set before consecutive treatments. PBS was instilled and stablished as the negative control (base line), to ensure that no alterations on the IOP were due to random conditions. Moreover, the positive control for IOP reduction was the marketed formulation above-mentioned before, since its effectiveness is already described in the clinical practice.

IOP pressure reduction (ΔIOP) was established as a parameter to evaluate the activity of the different treatments applied. Maximum percentage of ΔIOP (ΔIOPmax), onset time (t_{onset}), effective time ($t_{effective}$) as well as area under the ΔIOP (%)-time curve from 0 to the time at which ends the study (t') ($AUC_{0-t'}$) were determined for each sample evaluated and calculated by the lineal trapezoidal rule. Besides,

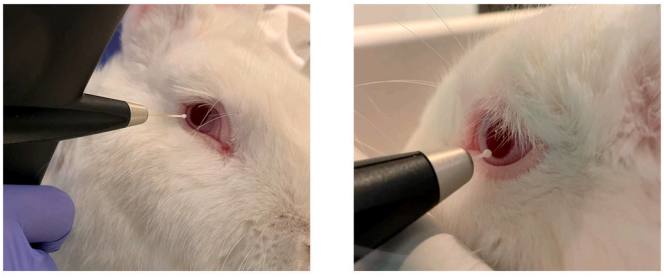

(A) (B)

Fig. 1. Method of determining IOPs of rabbits by using a Icare® Tonovet tonometer (Tiolat, Helsinki, Finland) from a far (A) and close approach (B).

bioavailability was assessed with 90% interval confidence according to the guidelines on investigation of bioequivalence [37].

2.8. Statistical analysis

Microemulsions were made and analyzed in triplicate (n = 3) and the data for *in vitro* experiments is shown as the mean ± SD. ImageJ2 2.3.0 (Fiji) was employed for cryo-TEM and SEM analysis. Fluorescence images were obtained and treated with ProgRes® CapturePro Satellite DLL 2.10.0 software. Finally, flow cytometry results were studied by Beckman Coulter Kaluza Analysis Software, US. Hypotensive curves described in the *in vivo* experiments are described as mean ± SEM and AUC graphs as mean ± SD. GraphPad software Inc. Prism Version 9, US, was used to perform Two-Way ANOVA for column comparison combined with Tukey test correction in cell viability studies. Furthermore, one-way ANOVA analysis in combination with Dunnett's test was employed to analyze the level of significance of cell viability between formulation at specific times, osmoprotective efficacy and AUC of IOP by using APA style (*; $p \leq 0.05$, **; $p \leq 0.01$, ***; $p \leq 0.001$ or ns; $p > 0.05$). Besides xy regression analysis was employed to obtain Y intercept and calculate detection and quantification limits. Furthermore, SPSS Statistics was used to analyze the influence of different parameters (eye, rabbit, and formulations) as well as the mean square error of the residuals in order to calculate bioavailability by means of a nested ANOVA.

3. Results

3.1. Physicochemical characterization

Hypotensive microemulsions with osmoprotective properties were characterized and compared to the physicochemical properties of human tears (Table 1). Sizes of nanodroplets for A-Lt and B-Lt were similar (21.37 ± 2.34 nm and 20.81 ± 2.56 nm respectively) with low polydispersity index (PDI). Microemulsion containing hyaluronic acid 0.2% (A-HA-Lt) increased its size over 10 nm up to 30.51 ± 3.20 nm. However, the addition of DXT (B-DXT-Lt) did not produce a change in the size (23.44 ± 5.34 nm) in comparison with A-Lt or B-Lt. Z potential was neuter in all cases (−10 to + 10 mV), although A-HA-Lt presented values close to 0 mV and B or B-DXT-Lt were slightly more negative than formulations including betaine and leucine with an without AH (−8.72 ± 0.48 mV and −6.76 ± 0.30 mV respectively). Regarding pH, all were neuter and suitable with the pH of the ocular surface (pH ≈ 7) except for the one with HA that decreased to 6.58 ± 0.01. Surface tension values of the microemulsions were between 34 and 36 mN m^{-1}, lower to those of the ocular surface (40–46 mN m^{-1}) [38] ensuring proper extensibility on the ocular surface. Regarding viscosity, A-Lt, B-Lt and B-DXT-Lt presented similar values to aqueous solutions and human tears at high shear rates (0.97 mPa s). As expected, A-HA-Lt viscosity resulted higher (>4-fold) than its analog without HA (A-Lt). Finally, osmolarity of the developed microemulsions loaded with latanoprost presented values close to the osmolarity of natural tears [39].

All Lt loaded microemulsions exhibited a unimodal distribution with narrow histograms, typical of microemulsion systems (Fig. 2). Microemulsion A-Lt exhibited less than 4% with sizes higher than 36 nm. Conversely, A-HA-Lt presented a frequency of 46% between 36 and 72 nm. B-Lt and B-DXT-Lt showed a 3.5% and 21.5% of sizes above 36 nm respectively.

Hypotensive formulations were visualized under Cryo-EM microscopy in order to assess and study morphological characteristics as well as inner structure (Fig. 3). Novel microemulsions presented uniform sizes, however A-HA-Lt microemulsions showed more homogeneous structures than formulation A-Lt. Calculated sizes of cryo-EM sizes were also useful to confirm DLS data. Furthermore, A-Lt microemulsion exhibited 19.72 ± 6.30 nm sizes while A-HA-Lt demonstrated vesicles sizes of 30.07 ± 4.96 nm. B-Lt showed 20.03 ± 4.15 nm sizes similar to A-Lt. Meanwhile the addition of dextran (B-DXT-Lt) did not change vesicle sizes 21.27 ± 3.11 nm.

SEM evaluation of osmoprotective microemulsion containing latanoprost showed that all microemulsions including latanoprost (A-Lt, A-HA-Lt, B-Lt and B-DXT-Lt) were homogeneous and similar in size. As previously described, formulation A nanodroplets sizes analyzed from SEM images showed 23.64 ± 7.39 nm while formulation A-HA-Lt increased sizes up to 31.32 ± 3.53 nm. Moreover, according to the images (Fig. 4) formulation B-Lt and B-HA-Lt were very similar in distribution, morphology and measured sized (23.09 ± 2.84 and 24.12 ± 3.03respectively). Besides images of the microemulsions containing amino acids (A-Lt and A-HA-Lt) were prone to exhibit charging phenomenon presenting some anomalous contrast.

3.2. Encapsulation efficiency

Latanoprost EE was quantified in the developed osmoprotective microemulsions (A-Lt, A-HA-Lt, B-Lt and B-DXT-Lt) and resulted ≥98%. This value was calculated taking into account the limit of detection and quantification of the calibration curve that were set at 0.93 μg/mL and 2.81 μg/mL respectively. Since no peak was detected in the filtrate, any possible concentration would be lower than the detection limit which entails 1.9% over the total latanoprost. Therefore, when latanoprost is not detected ≥98% of encapsulation efficiency can be ensured (Table 2).

3.3. In vitro cell tolerability

Cell tolerance of hypotensive microemulsions (A-Lt, A-HA-Lt, B-Lt, B-DXT-Lt) were evaluated in HCECs and HConEpiCs for different time periods (1h and 4h) (Fig. 5). All hypotensive microemulsions presented cell viabilities higher than 80% in both cell lines tested [30]. A-Lt and A-HA-Lt formulations presented the highest tolerance values at 1 h exposure (102.81 ± 11.36% and 113.40 ± 13.86% respectively). At 4 h exposure, those containing polymers (A-HA-Lt and B-DXT-Lt) exhibited greater values (101.69 ± 17.31% and 92.92 ± 11.58) than formulations without polymer addition (86.14 ± 9.49% for A-Lt and 86.96 ± 0.56) for B-Lt respectively) although no significant differences were found ($p < 0.05$). Regarding *in vitro* tolerance in HConEpiCs, all formulations had similar values (≈94–100%) at 1 h exposure while longer exposure (4h) showed higher viability values for A-Lt and A-HA-Lt (96.48 ± 5.61% and 96.01 ± 1.89%) than for B-Lt and B-DXT-Lt respectively (83.81 ± 2.14% and 86.52 ± 1.97%) following all the acceptance criteria (viability values > 80%). Conversely, marketed formulation (Monoprost®) showed poor viability values at 1h in cornea and conjunctiva (51.82 ± 8.65% and 50.59 ± 8.21%) respectively and even less at 4 h of exposure (38.42 ± 4.13% and 24.09 ± 3.64%respectively).

Table 1
Characterization of hypotensive latanoprost microemulsions in terms of size, PDI, zeta potential, pH, surface tension, viscosity and osmolarity.

	Nanodroplet Size (nm)	PDI	Zeta potential (mV)	pH	Surface tension (mN·m^{-1})	Viscosity (mPa·s)	Osmolarity (mOsm/L)
A-Lt	21.37 ± 2.34	0.01	−2.57 ± 0.24	7.04 ± 0.02	34.70 ± 0.44	1.13 ± 0.09	281.49 ± 3.69
A-HA-Lt	30.51 ± 3.20	0.01	−0.03 ± 0.07	6.58 ± 0.01	36.77 ± 0.55	4.58 ± 0.08	283.43 ± 5.21
B-Lt	20.81 ± 2.56	0.01	−8.72 ± 0.48	7.43 ± 0.01	35.93 ± 0.29	1.22 ± 0.07	278.83 ± 1.87
B-DXT-Lt	23.44 ± 5.34	0.05	−6.76 ± 0.30	7.10 ± 0.01	36.87 ± 0.56	1.30 ± 0.04	288.80 ± 2.15

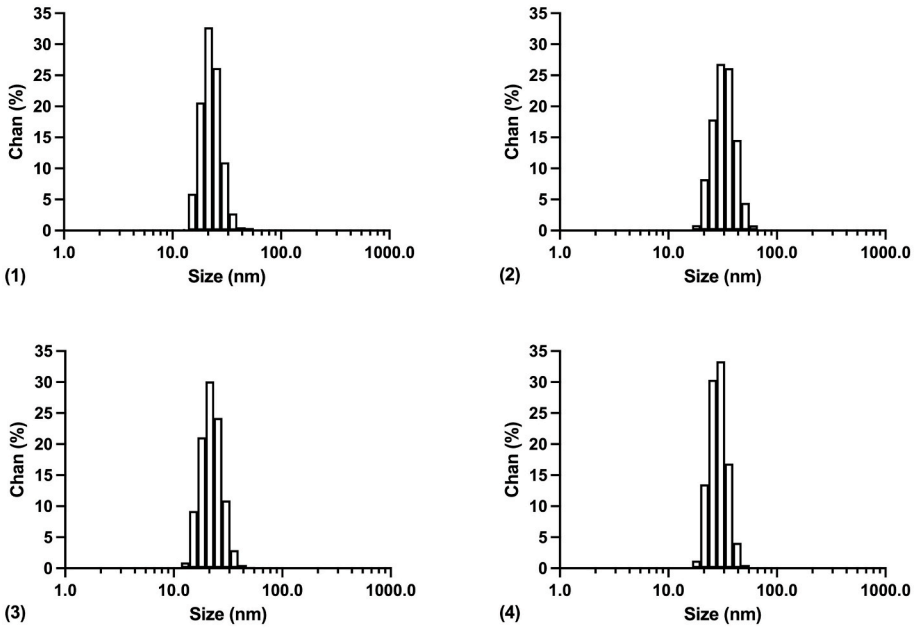

Fig. 2. Size distribution of the hypotensive microemulsions developed with osmoprotective properties (1), (2), (3) and (4) for A-Lt, A-HA-Lt, B-Lt and B-DXT-Lt respectively.

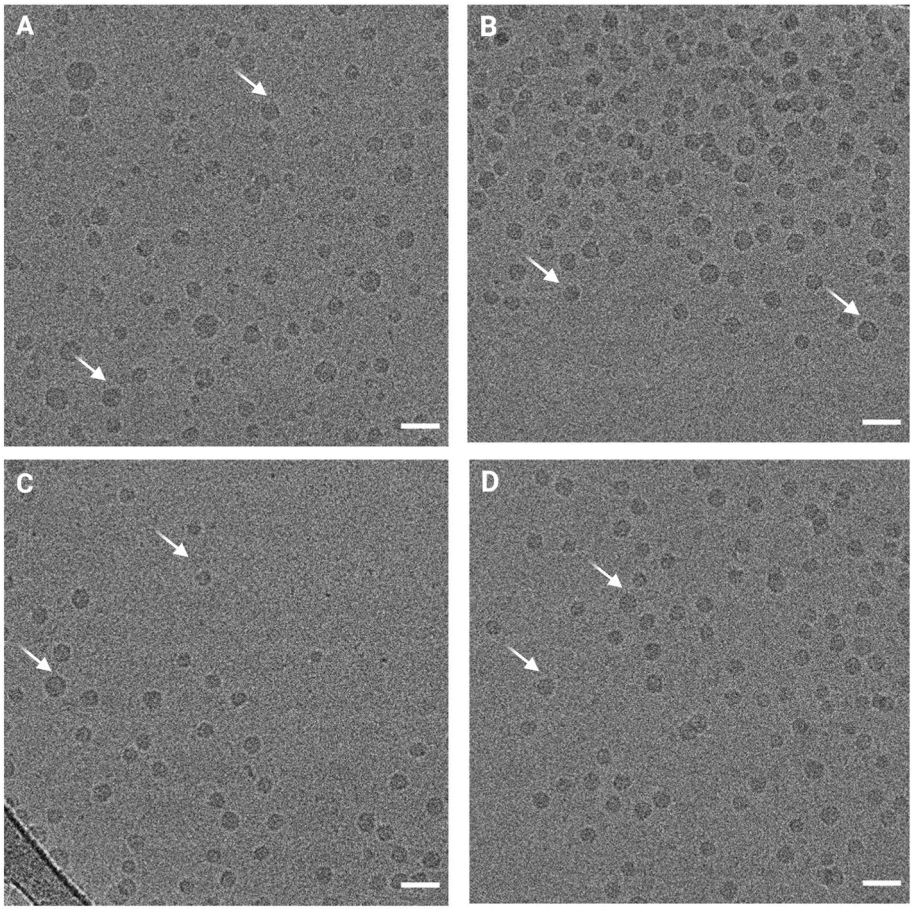

Fig. 3. Cryo-TEM microscopy displaying hypotensive microemulsions A-Lt (A), A-HA-Lt (B), B-Lt (C) and B-DXT-Lt (D). Some nano-drops are illustrated (arrows) and the scale bar is set at 50 nm.

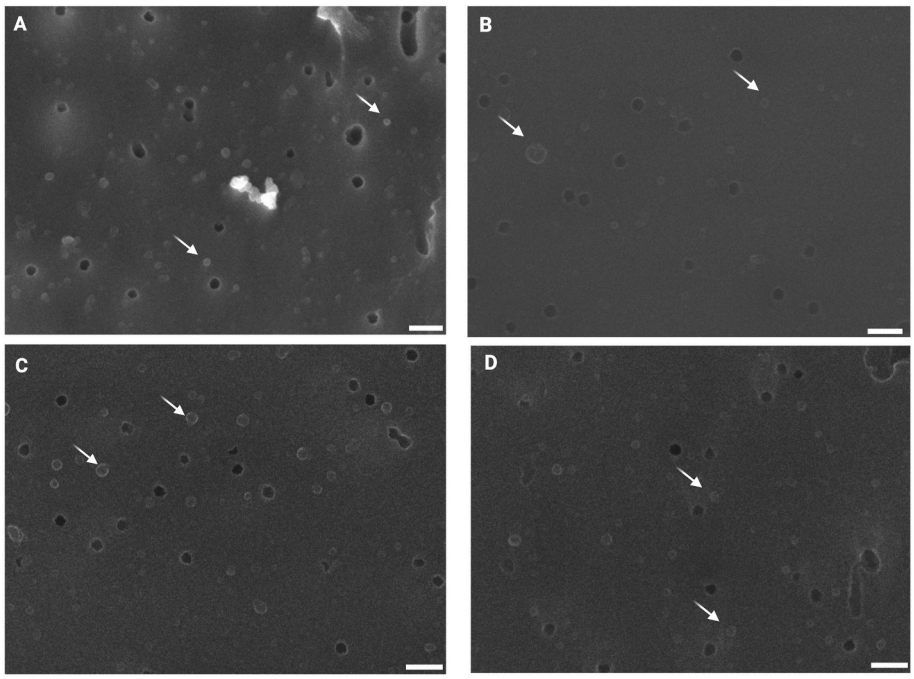

Fig. 4. SEM images showing some groups of microemulsions developed (A-Lt, A-HA-Lt, B-Lt and B-DXT-Lt illustrated in A, B, C and D respectively with a scale bar of 200 nm.

Table 2
Latanoprost yield and EE quantification in osmoprotective hypotensive microemulsions. *ND: Non detected presenting a concentration lower than the limit of quantification.

Formulation	Total concentration (μg/mL)	Yield (%)	Ultrafiltrate concentration (μg/mL)	EE (%)
A-Lt	45.78 ± 0.65	91.55 ± 1.31	ND	≥98%
A-HA-Lt	45.18 ± 0.75	90.36 ± 1.50	ND	
B-Lt	46.44 ± 1.04	92.89 ± 2.08	ND	
B-DXT-Lt	47.65 ± 0.73	95.31 ± 1.46	ND	

3.4. Osmoprotective efficacy in cellular model of hyperosmolarity

Osmoprotective efficacy of the hypotensive microemulsions was assayed in a hyperosmolar stress model in HCECs. All formulations exhibited significant osmoprotective activity after 2 h exposure ($p < 0.001$). Cells in contact to hyperosmolar environment (470 mOsm/L) without previous osmoprotective exposure showed viability values of 19.75 ± 4.91% (positive control) while the viability values are increased to 44–60% (2-3-fold more) when cells were pretreated with the osmoprotective microemulsions (Fig. 6). A-Lt showed higher osmoprotective efficacy than A-HA-Lt (58.85 ± 1.41% and 51.24 ± 1.63% respectively) without statistical differences. B-Lt and B-DXT-Lt osmoprotective values were also similar without significant differences (47.10 ± 4.91% and 43.94 ± 3.37% respectively). Furthermore, no differences were found when comparing the different formulations (A-Lt and B-Lt).

3.5. Permeation studies

3.5.1. Microscopy

Non loaded microemulsion and in combination with polymers (HA and dextran) containing coumarin were incubated with HCECs for 5 min as previously mentioned and their mean fluorescence was monitored

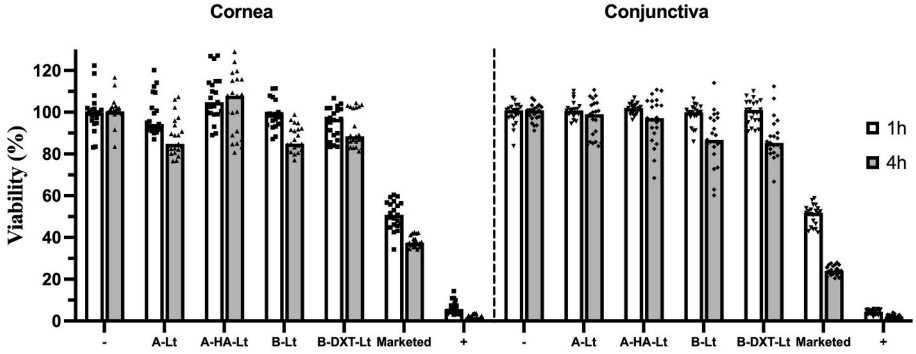

Fig. 5. *In vitro* tolerance of osmoprotective hypotensive microemulsions in HCECs and HConEpiCs at different exposure times (1h and 4h) in comparison with the marketed one (Monoprost®), negative control (-; untreated cells) and positive control (+; BAK 0.005%).

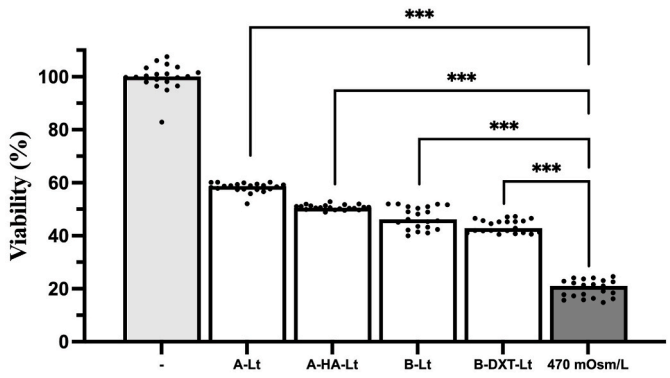

Fig. 6. Osmoprotective preventive efficacy of developed microemulsions with latanoprost under a hyperosmolar environment.

and determined for 11 days. All formulations showed a remarkable peak of intensity at day 0 with a decrease in time up to 11 days when almost all fluorescence has disappeared. BM-HA images (Fig. 7) showed a fluorescent intensity higher than BM and BM-DXT respectively at day 0 and 2. Besides, cells when exposed to BM-HA showed fluorescence longer than BM and BM-DXT. BM and BM-DXT showed similar fluorescence although BM-DXT seems have slightly more fluorescence than BM. BM images almost showed a completely disappearance in fluorescence at day 9.

Regarding calculated CTCF BM-HA demonstrated remarkable fluorescence peak at day 0 higher (333265.31 ± 32391.85) than BM and BM-DXT respectively (Fig. 8) ($p < 0.01$). Besides mean fluorescence of BM-HA was significantly higher (51931.83 ± 7531.89) than BM and BM-BM-DXT (7417.51 ± 2640.59 and 26702.10 ± 12403.22 respectively) up to 9 days reaching similar results at the end of the study (day 11). Conversely BM and BM-DXT presented similar values of CTCF in all images with slightly increases at 2, 6 and 9 days without significant differences.

3.5.2. Flow cytometry

Flow cytometry experiments showed the evolution of fluorescence within 11 days after exposition to blank microemulsions (BM, BM-HA, BM-DXT). Similarly, to the results obtained with CTCF from the images, BM-HA and BM-DXT exhibited higher mean fluorescence at 0, 2, 4 and 7 days than BM as can be seen in Fig. 8. Besides, maximum peak of fluorescence at day 2 for BM-HA (515.28 ± 12.12) and BM-DXT (356.50 ± 10.85) were higher than the ones obtained for BM (172.94 ± 13.96). Besides, BM-HA and BM-DXT showed maximum peaks at 4 days (220.53 ± 8.47 and 256.25 ± 7.03 respectively) and 7 days (252.09 ± 4.56 and 226.28 ± 8.19 respectively) superior to BM (67.41 ± 4.8 for 4 days and 43.02 ± 3.17 for 7 days). Finally, fluorescence at day 11 was superior in those containing polymers although all of them were almost negative in FL1 signal (10^0) (Fig. 9).

3.6. Cell-Microemulsion interactions

3.6.1. Scanning electron microscopy

Morphology of HCECs exposed to microemulsions was assessed in the SEM as previously described (Fig. 10). Cells without any treatment exposed to NaCl 0.9% (control) exhibited normal morphology with few common membrane pores. An increase of pore numbers of different sizes in the cell membranes were observed after exposure to latanoprost microemulsions (A-Lt, A-HA-Lt, B-Lt, B-DXT-Lt). Those exposed to A-Lt presented an average pore size of 74.40 ± 16.43 nm with regular shapes while A-HA-Lt presented bigger pore sizes with irregular distribution (139.27 ± 13.07 nm). B-Lt showed irregular pattern of membrane pores in some regions with an average size of 104.61 ± 29.01 nm whereas B-DXT-Lt exhibited smaller pore sizes (56.21 ± 3.06 nm) with a conserved distribution.

It is also worth mentioning that in all images microemulsión droplets could be appreciated entering corneal epithelial cells by opening small nanometric pores through the cell membrane which were not present in untreated cells. It was also observed that those containing Polymers (A-HA-Lt and B-DXT-Lt) seemed to be more aggregated in some specific membrane regions than those without mucoadhesive polymers. Moreover, nano droplets were particularly abundant and localized on cell protrusions and pseudopodia in cell surroundings.

3.6.2. Transmission electron microscopy

TEM was employed to analyze the interaction between microemulsions and the inner structures of HCECs as well as their cellular distribution in the ultrathin cellular sections (Fig. 11). Control cells exposed to NaCl 0.9% (untreated) presented a normal appearance showing empty vacuoles and clear fields of the cytoplasm. Regarding microemulsions containing latanoprost, clear lipid deposits associated to microemulsions internalization were appreciated in the darkest tone (black arrows). Most of them were located in vacuoles creating reservoir-like structures. Formulations without polymers (A-Lt and B-Lt) showed a higher number of oily deposits than those containing polymers (A-HA-Lt and B-DXT-Lt). In addition, individual particles (microemulsion droplets) can be seen across the cytoplasm and particularly concentrated in the surroundings of vacuoles and inner cellular membranes. These, are particularly intense dark-colored and well defined in the case of A-AH-Lt. Moreover, these nano-droplets (20–30 nm) tend to pass across inner cellular membranes such as the nuclear one. A-Lt and B-Lt can be identified inside nucleus and B-Lt specifically passing through the cellular membrane. Generally, microemulsions were also localized in mitochondria although in a lesser extent and particularly concentrated close to the marginal side of cellular membrane.

3.7. Hypotensive efficacy

Hypotensive effect of developed microemulsions with latanoprost (A-Lt, A-HA-Lt, B-Lt, B-DXT-Lt) and marketed formulation (Monoprost®) was measured. Hypotensive activity of non-loaded microemulsions was also tested (BM, BM-HA and BM-DXT). PBS (control) was instilled and IOPs monitored to ensure that no hypotensive effect was given. Moreover, unloaded microemulsions (blank) showed an intrinsic hypotensive effect for 24h that was increased for the formulations including polymers (BM-HA and BM-DXT) being similar to the effect observed in the marketed formulation (Fig. 11). While marketed formulation exhibited a ΔIOPmax of 19.70 ± 9.49%, BM-HA and BM-DXT showed values of 18.15 ± 6.20% and 14.53 ± 7.86% respectively. Conversely, BM showed lower ΔIOPmax values (8.27 ± 4.99%) than marketed one although showing some level of hypotensive activity between 3h and 10h ($p < 0.05$) (Fig. 12). Furthermore BM-HA demonstrated hypotensive activity between 3h and 36h while marketed one (between 1h and 30h).

Regarding latanoprost loaded microemulsions developed in this work, hypotensive activity in rabbits was substantially higher in comparison with the marketed one (Fig. 13). While hypotensive activity for marketed formulation lasted for 24h–30h, the activity of A-Lt lasted for 82h (3.42 days). Besides, the addition of hyaluronic acid (A-HA-Lt) prolonged its hypotensive activity up to 310h (12.92 days). Moreover B-Lt lasted for 130h (5.42 days) while the addition of dextran lasted for 202h (8.42 days). ΔIOPmax were higher in comparison with the marketed one. One the one hand A-Lt and A-HA-Lt showed ΔIOPmax of 24.24 ± 7.09% and 34.16 ± 5.67% respectively. On the other hand, B-Lt exhibited a ΔIOPmax of 22.55 ± 3.96% while B-DXT-Lt showed an ΔIOPmax of 25.40 ± 4.25%. ΔIOPmax for A-HA-Lt resulted significantly higher in comparison with marketed formulation ($p < 0.05$). Although the rest of formulations were not significantly different in terms of ΔIOPmax in comparison with the marketed formulations the hypotensive activity, area under the curve and relative biodisponibility was

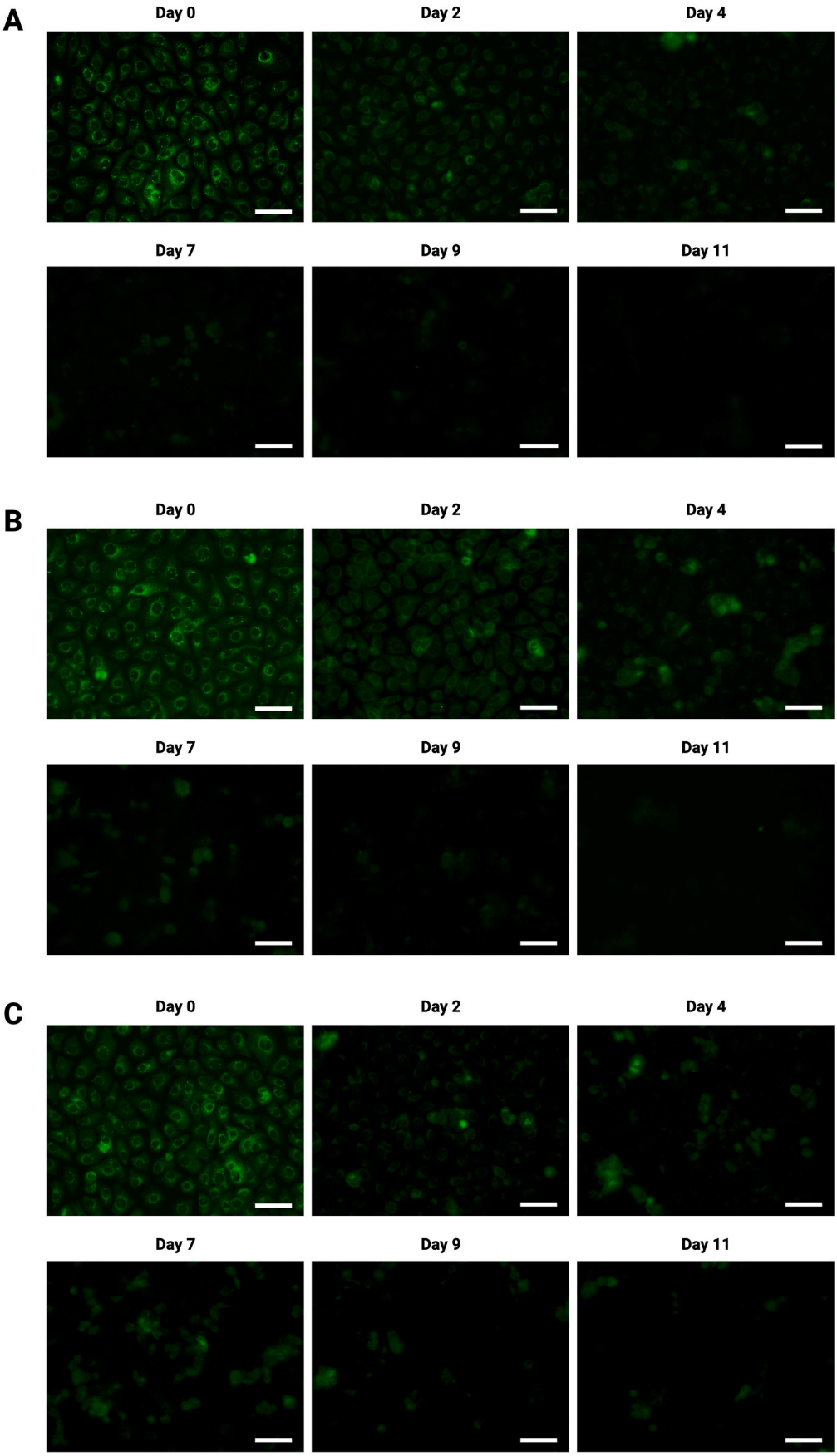

Fig. 7. Fluorescence images showing internalization of BM (A), BM-HA (B) and BM-DXT (C) in HCECs lasting for 11 days after 5 min exposure (50 μm scale bar).

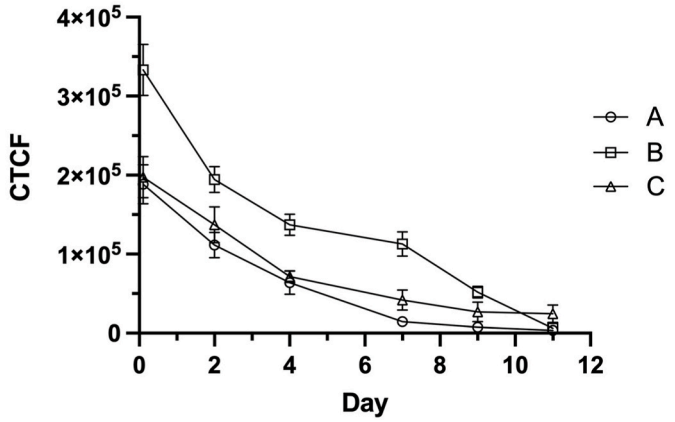

Fig. 8. Corrected total cell fluorescence (CTCF) of BM (A), BM-HA (B) and BM-DXT (C) respectively for 11 days.

much higher (Table 3) and statistically significant.

Regarding calculated $AUC_{(0\text{-}t')}$, all the developed formulations with and without latanoprost were compared with the marketed formulation (Monoprost®) (Fig. 14). Firstly, for those developed microemulsions without latanoprost, BM-HA was similar to the marketed formulation in terms of hypotensive effect ($p > 0.05$). $AUC_{(0\text{-}t')}$ of microemulsions without polymers (A-Lt and B-Lt) were much superior (65.73 ± 12.48 and 73.58 ± 19.36 respectively) than marketed formulation (13.52 ± 4.83) ($p < 0.001$). Generally, all microemulsions containing latanoprost were very significant in comparison with the marketed one ($p < 0.001$). Particularly the addition of HA increased the $AUC_{(0\text{-}t')}$ from 65.73 ± 12.48 (A-Lt) up to 271.50 ± 38.15 (A-HA-Lt) ($p < 0.001$). It is also worth noting that dextran increased $AUC_{(0\text{-}t')}$ from 73.58 ± 19.36 (A-Lt) to 157.40 ± 37.84 (A-DXT-Lt) ($p < 0.01$) as can be seen in Table 3.

Finally, relative bioavailability (RB) calculated from AUC (0-t') data, demonstrated that the microemulsions of the present study showed superior results in comparison with the marketed formulation employed as reference. A-Lt exhibited an average RB value of 4.52 times higher than the reference while the addition of the mucoadhesive polymer, HA made the difference 18.55 times higher than the control formulation. With regards to formulation B-Lt, RB value showed 5.11 times more than marketed one, increasing to 10.50 times more when dextran was added.

4. Discussion

The design of novel systems and therapeutical strategies that increase residence time of drugs (both lipophilic and hydrophilic) as well as enhance their permeation through different ocular tissues is a technological challenge [40]. Besides, formulations tolerability is a critical point to be considered. Regarding topical formulations, a relevant number of existing hypotensive formulations for glaucoma treatment include different excipients, mainly preservatives, that affect the ocular surface integrity or produces adverse effects such as ocular surface discomfort, dryness, or hyperemia hampering patient adherence [4]. In addition, some of these formulations including active substances such as certain hypotensive drugs or preservatives could be responsible for different side effects [41]. Furthermore, a combination of different anti-glaucoma drugs as well as repeated administrations is needed in most cases to achieve a suitable IOP control [42]. All these issues (preservatives, repeated doses, and drugs combinations) bring to evidence the need of novel therapies to overcome side effects when managing glaucoma. Nowadays, new therapies are expected to be not only well tolerated but also include protective substances with the ability to preserve the ocular surface integrity against harmful potential effects. For that reason, in this study we tried to develop topical ophthalmic pharmaceutical nanosystems (microemulsions) including a hypotensive drug (latanoprost) accompanied by osmoprotective substances and in combination with mucoadhesive polymers. The purpose of such, was extending the ocular surface contact time providing protection while delivering anti-glaucoma therapy. O/W microemulsions containing some others antiglaucoma drugs have been previously developed by some authors. This is the case of brimonidine tartrate in a microemulsion (90–100 nm nanodroplet size) with high viscosity values [43]. Other authors prepared bimatoprost microemulsions made out of isopropyl myristate and tween 20 (25–30 nm droplet size and neuter z potential) to be included in contact lenses [44]. Besides and in contrast to ordinary emulsions previously prepared by some authors [45] microemulsions are more efficient and stable nanosystems with highly potential benefits for the treatment of ocular diseases.

Ophthalmic microemulsions developed by self-emulsification through low energy methods have been previously developed by our group with osmoprotective properties [32]. They have been able to protect corneal cells from hyperosmolar stress for the treatment of ocular surface diseases that develop with hypertonic stress such as DED. In the present work, latanoprost has been loaded in an osmoprotective microemulsion with a very low concentration of surfactants (1,5%) showing nanodroplet sizes around 20 nm which were increased to around 30 nm with the inclusion of hyaluronic acid. All formulations presented neuter pH values (6.5–7.5) and almost isotonic values (278–290 mOsm/L). The low surface tensions obtained in the different formulations guarantee a good extension onto the ocular surface and the addition of mucoadhesive polymers enhance their residence time [46].

According to the above-mentioned studies, Cryo-TEM and SEM visualization showed that all formulations developed in this work had very conserved sphere-like morphology as should be, according to other authors [20]. In all formulations, the inclusion of latanoprost and osmoprotective substances did not affect their morphology. Some authors have visualized microemulsions at regular TEM showing nanodroplets of 90–100 nm using negative staining [47]. However, for lipid-based nanosystems and in particular nano- and microemulsions this can be problematic since environmental modifications and conditioning of the sample can affect these systems stability. For that reason, one of the most appropriate techniques for their visualization is

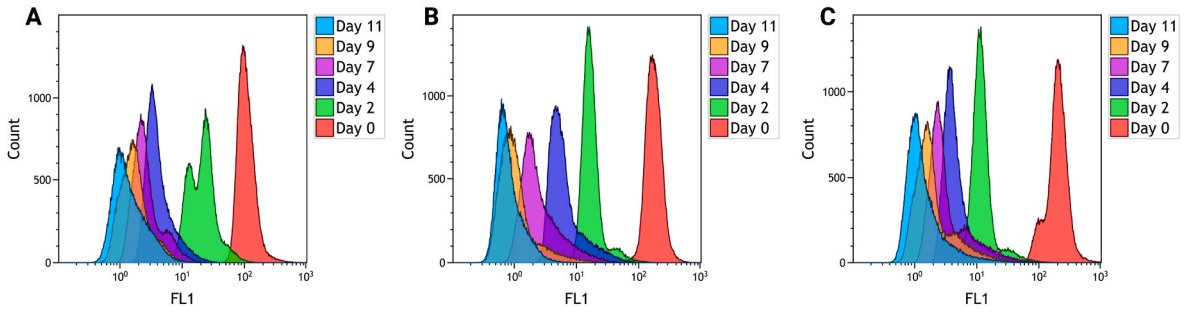

Fig. 9. Flow cytometry histograms showing cell count vs fluorescence intensity (FL1) in logarithmic scale at different shown periods of BM (A), BM-HA (B) and BM-DXT (C).

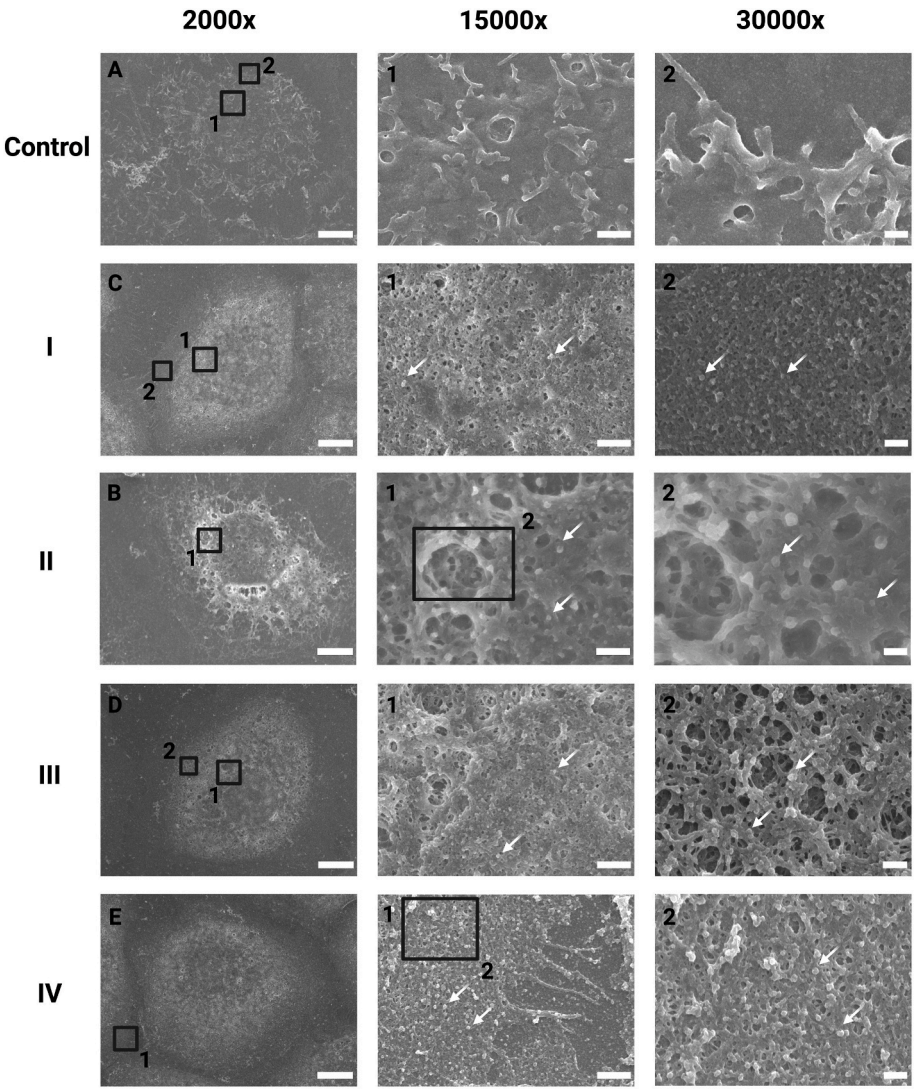

Fig. 10. SEM images of HCECs exposed to no treatment (control) and cells exposed for 5 min to the developed formulations A-Lt, A-HA-Lt, B-Lt and B-DXT-Lt (I, II, III and IV respectively). Different augments were employed to assess cell microemulsion interactions (x2000: 8 μm, x15000: 1 μm and x30000: 200 nm scale bars). Microemulsions are indicated clearly by white arrows close to pore membranes.

cryo-TEM [48,49]. We showed that cryo-TEM did not modify sizes since a modification of the environment is not artificially changed, being nanodroplet sizes similar to those analyzed with DLS. Besides, we used a protocol of staining for SEM morphology visualization [33] with some modifications by combining green malachite, commonly known for its ability to fixate lipids with glutaraldehyde [50].

We also assessed the ability of the developed microemulsions to entrap the hypotensive prostaglandin latanoprost. All the microemulsions showed yields higher than 90% and encapsulation efficiencies close to 100%. We hypothesized that the 10% prostaglandin lost could be lost due to the small amount (10 μL) added from the ethyl oleate latanoprost solution during the microemulsion preparation. The results are similar to the ones obtained by other authors encapsulating travoprost in a nanoemulsion confirming that the lipophilic substances could be successfully included in these pharmaceutical systems [51].

The currently developed hybrid osmoprotective microemulsions loaded with latanoprost showed good *in vitro* tolerance in both, corneal and conjunctival epithelial cell cultures under conditions previously established by our group to simulate *in vitro* chronic administration of topical ophthalmic formulations [31]. According to other authors, the poor tolerability obtained (close to 50% after 1h and 20–30% after 4h in both corneal and conjunctival cells) under such conditions for the marketed formulation Monoprost® could be attributed to the high percentage of hydrogenated castor oil (5%) [52] in combination with long-term toxicity of latanoprost [53]. In the present work, we have included a combination of osmoprotective substances (leucine/betaine or clusterin/oleanolic acid) in two different types of formulations with and without mucoadhesive polymer addition (hyaluronic acid for A-HA-Lt or dextran for B-DXT-Lt) with the idea of protecting the ocular surface in chronic treatments. To test our hypothesis, we study cell survival of the developed formulations under a hypertonic stress cellular model previously published by our group [30]. In this model, cellular viability decreased to values lower than 20% after exposure to a hyperosmolar solution (470 mOsm/L) in untreated cells. Then, to test the protective ability of previous osmoprotective microemulsions, corneal cells were previously exposed to each formulation followed by hyperosmotic stress simulation once treatments had been removed. In all microemulsions, an increasement in cell survival resulted in 25–40% compared with the untreated control under hypertonic conditions. In fact, osmoprotective formulations containing latanoprost showed 2-3-fold of cell survival (treated) more than the positive control (untreated). Therefore, we hypothesized that these hybrid microemulsions not only exhibit the ability to increase cell tolerance and decrease toxicity associated to latanoprost but also to avoid cell death induced by

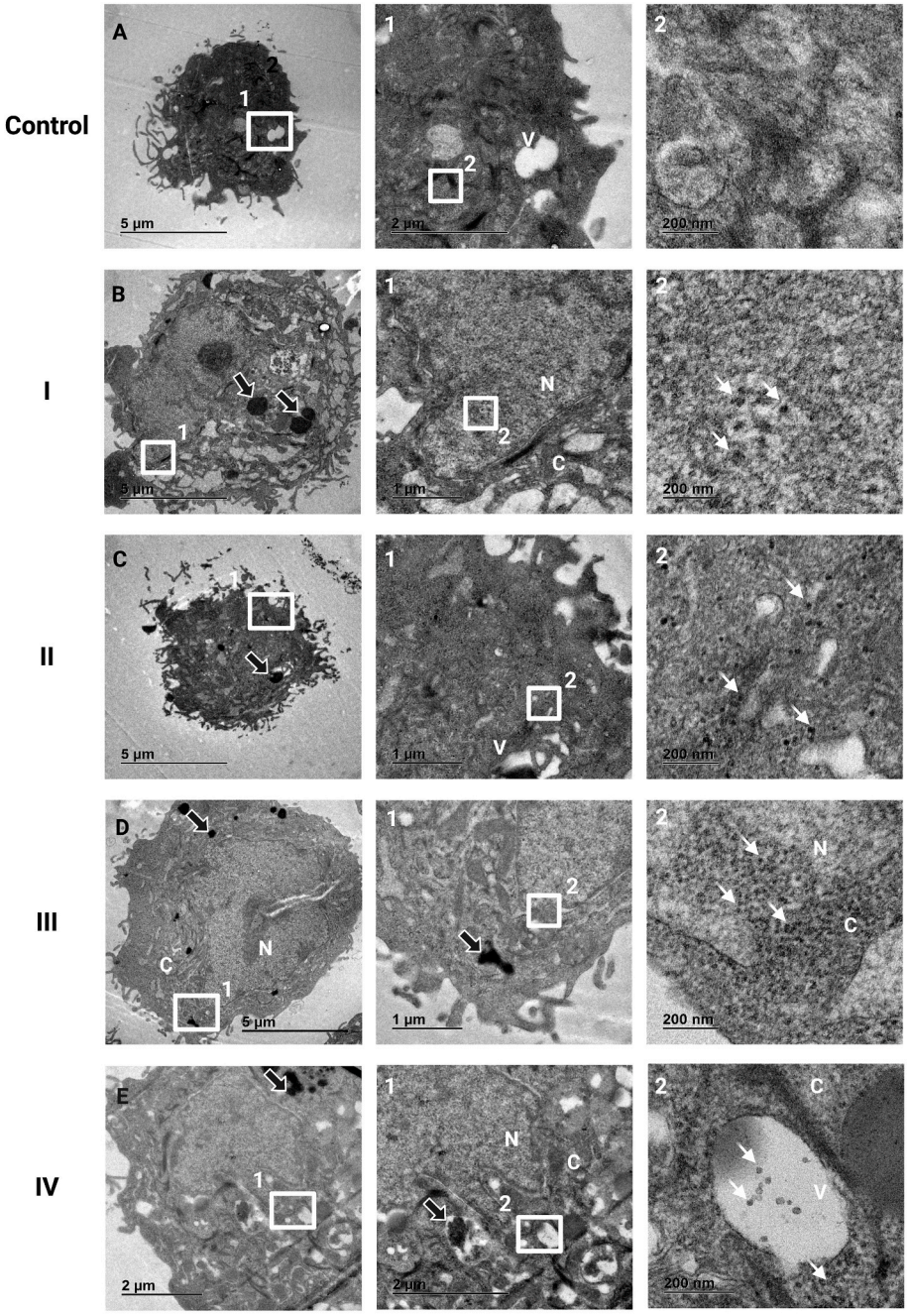

Fig. 11. TEM images of HCECs unexposed cells (control) and cells exposed for 5 min to the developed formulations A-Lt, AHA-Lt, B-Lt, and BDXT-Lt (I, II, III and IV respectively). Different augments were employed to assess cell microemulsion interactions in different cell structures (C: cytoplasm, V: vacuole and N: nucleus). All formulations were visualized at 8000x and zoomed 30000x and 150000 (1 and 2 respectively) except for IV that was zoomed at 150000x (1 and 2). Black arrows represent lipid deposits while white arrow single microemulsions.

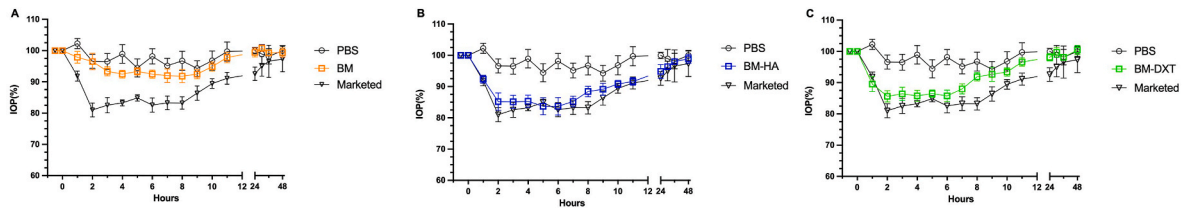

Fig. 12. Intrinsic hypotensive effect of model developed microemulsions BM (A), BM-HA (B) and BM-DXT without latanoprost in comparison with the marketed formulation.

chronic hypertonic environment with only 2 h of pre-exposure. In previous studies performed by our group, betaine and hyaluronic acid have demonstrated to be highly protective to cell shrinkage, inflammation and apoptosis induced by hypertonic environment [30].

To confirm the ability of internalization of the microemulsions in corneal cells, blank microemulsions (BM, BM-HA and BM-DXT) were loaded with fluorescence coumarin. HCECs exposed to coumarin-loaded microemulsions at 2 μg/mL for a short time (5 min) demonstrated a high

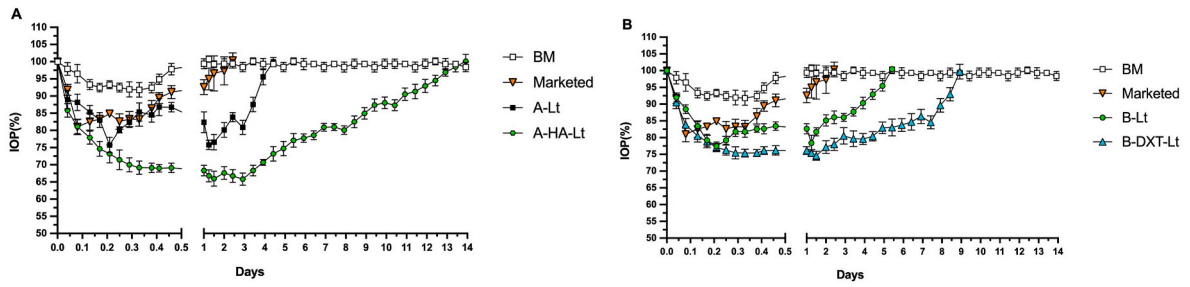

Fig. 13. Comparison of hypotensive developed formulations containing latanoprost A-Lt, A-HA-Lt (A), B-Lt, B-DXT-Lt (B) with BM and marketed formulation.

Table 3
Microemulsions developed showing ΔIOPmax, $AUC_{(0\text{-}t')}$ and relative bioavailability (RB) representing confidence intervals.

Formulation	ΔIOP_{max} (%)	$AUC_{(0\text{-}t')}$ **(%.h)**	RB[a]
Marketed	19.70 ± 9.49	13.52 ± 4.83	1
A-Lt	24.24 ± 7.09	65.73 ± 12.48	4.52 (4.01 – 5.32)
A-HA-Lt	34.16 ± 5.67	271.50 ± 38.15	18.55 (17.42 – 19.96)
B-Lt	22.55 ± 3.96	73.58 ± 19.36	5.11 (4.55 – 5.97)
B-DXT-Lt	25.40 ± 4.25	157.40 ± 37.84	10.50 (9.62 – 11.67)

[a] Relative bioavailability is expressed in times superior to reference formulation with 90% significance ($p = 0.01$).

internalization activity. The assessed fluorescence showed that HA containing microemulsions exhibited higher fluorescence retention time than BM and BM-DXT overtime as well as presenting residual fluorescence up to 11 days after one single instillation. Interestingly, exposure time for this studies (5 min) resulted lower than other employed by some authors (60 min) using coumarin-loaded liposomes (20 μg/mL) to assess internalization efficacy of an anti-inflammatory liposomal formulation [54]. The results obtained by fluorescence were confirmed by flow cytometry. The polymers included in the formulations (HA and dextran) seemed to increased retention time. These findings indicate these polymers entail interesting biomaterials to promote penetration of encapsulated active drugs in microemulsions.

The modified SEM protocol in combination with PFA previously described for lipid visualization [33] was employed to assess interactions between osmoprotective microemulsions loaded with latanoprost and cell membranes. PFA has been previously used in SEM studies with macrophages and gold nanoparticles [55]. According to SEM images, an increase of pore numbers in cell membranes were observed after hypotensive microemulsions exposure (Fig. 10). According to other authors these reversible pore formation could be due to the surfactant concentration used to stabilize the nanodroplets [56]. Nevertheless, it is important to take into account that the small size of nanodroplets probably allows enhanced penetration in cells through natural occurring pores and avoid endosomal formation which increase internalization rate and efficacy. It is important to remark that there are previous studies in which cell distribution has been studied by TEM [57]. However, they were performed without lipid specific fixation. To our knowledge, this is the first study to show cell-microemulsion interaction and in particular in human corneal epithelial cells. In the present work, *in situ* fixation of lipid nanodroplets (20–30 nm) at the moment of internalization allow to visualize the inner structures of the cell. As previously shown, vacuoles and cytoplasm of untreated cells are clear with structures associated with cellular physiological conditions. Regarding those exposed to hybrid microemulsions developed, intense lipid fixation inside vacuoles is present which can be explained by microemulsions accumulation allowing their release overtime. Moreover, fixed individual nanodroplets are visualized along the different cellular structures (vacuoles, nucleus, cytoplasm, endoplasmic reticulum, mitochondria, and cell membrane) although they are particularly concentrated on the surrounding of vacuoles.

All these findings support the high hypotensive effect assessed *in vivo*. Surprisingly, blank microemulsions exhibited hypotensive activity and even the one with HA presented the same pattern than the marketed formulation ($p > 0.05$). We contemplate the possibility of an intrinsic hypotensive effect of the developed formulations due to the high amount of lipidic compounds with unsaturated fatty acids present on the

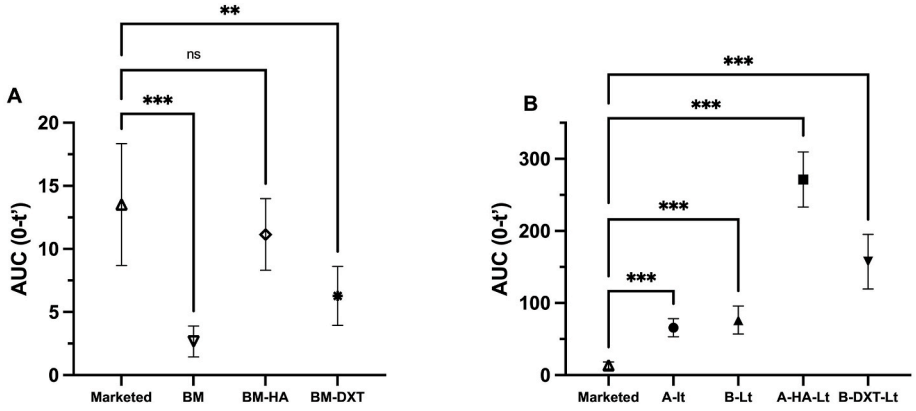

Fig. 14. AUC until effectiveness of the formulations (AUC 0-t') without latanoprost (A) and those containing latanoprost in comparison with the marketed formulation (B).

formulation (ethyl oleate, soybean oil, soy phosphatidylcholine and squalene). In fact, Bellenger-Germain et al. showed already the antihypertensive activity of rich fatty acid in hypertensive rats [58]. Also, Nowacki et al. established a direct relation between unsaturated fatty acids (specially lecithin derived) and the regulation of high-conductance Ca^{2+} activated potassium channels (BK) of vascular smooth muscles [59]. Furthermore, other studies assess the importance the presence of smooth muscles in the trabecular meshwork [60] and their regulation in aqueous blood flow pathways [61]. In addition, Cuppoletti et al. showed the ability of the prostaglandin analogue unoprostone to activate BK channels present in Schlemm's canal involved in volume regulation which contributes to lowering IOP and increasing aqueous humour outflow [62]. We speculate that due to the high and fast internalization rate of the developed microemulsions, they are able to reach the trabecular meshwork and according to the above-mentioned mechanisms in the literature, activate BK channels thus lowering the IOP. Therefore, this could be the first study to describe a hypotensive effect produced by unsaturated fatty acids in the eye. No effects other than osmoprotection and possible IOP decrease were described for the rest of the raw materials of the formulation. In any case, further studies are necessary to explain this intrinsic effect currently under study by our group. Microemulsions loaded with Latanoprost (A-Lt and B-Lt) resulted effective after one single instillation up to 4 and 6 days respectively with slightly higher values of ΔIOPmax (%). The hypotensive effect observed resulted longer than the one described by other authors. Xu et al. described a reduction for 72h and 96h in New Zealand rabbits with a bimatoprost-loaded microemulsion in contact lenses with 50 μg/mL and 75 μg/mL latanoprost concentrations respectively [44]. Moreover, according to the $AUC_{(0\text{-}t')}$, A-Lt and B-Lt were significantly higher in comparison with the commercial formulation. Besides, calculated relative bioavailability was 4.52 (4.01–5.32) and 5.11 (4.55–5.97) times more for A-Lt and B-Lt respectively than the marketed formulation.

After the addition of one single drop (25 μL) in each eye with A-HA-Lt, hypotensive effect lasted for almost 13–14 days, exhibiting a high increase in the hypotensive activity (34.16 ± 5.67% ΔIOPmax). A-HA-Lt showed superior values of RB (18.55 times more; CI90%: 17.42–19.96) than the marketed one. Dextran did also show long hypotensive values (lasting for 8–9 days) and exhibiting RB of 10.50 (9.62–11.67) times higher in comparison with the reference. This in the line of previous studies that developed prostaglandin nanoemulsions with multiple dose administration for the treatment of glaucoma [63].

It is important to highlight that currently there is not any hypotensive formulation present in the market that combine ocular surface protection and such long-lasting action as the one presented in this work. In this sense, all these novel findings suggest that the combination of the studied osmoprotective agents in this novel microemulsion technology loaded with latanoprost could entail a new and ground-breaking tool in the treatment of glaucoma. It has been demonstrated that the addition of mucoadhesive polymers enhance the benefits of the formulation. All these factors (tolerability, suitable physicochemical properties, osmoprotection, internalization capacity and long-lasting hypotensive effects) would increase patient adherence, improving effectiveness and quality of life by avoiding excessive repeatedly dose administrations as well as drug combinations eventually leading to ocular adverse effects (DED, hyperaemia, discomfort, and poor adherence). Moreover, previous studies conducted by our group confirmed the good stability (physiochemically and *in vitro* cell tolerability) under refrigerated conditions almost for one year as well as the *in vivo* tolerability of these type of formulations [32]. The developed microemulsion could be employed for future ocular therapies increasing the residence time and permeation of therapeutic agents (both hydrophilic and lipophilic) for long periods of time to the desired tissues. However, an animal model of ocular hypertension as well as detailed pharmacokinetic studies would be interesting to confirm this promising results.

5. Conclusions

The present work, studied the development of a new self-emulsifying microemulsion system displaying high cell permeability and distribution, good tolerance, and suitable physicochemical properties for topical ophthalmic administration. The addition of combined osmoprotective substances in a prostaglandin-loaded microemulsion entails a novel strategy for the treatment of glaucoma and management of ocular surface diseases associated to chronic hypotensive therapies. Besides, developed microemulsions with mucoadhesive polymers provide a remarkable long-term activity after one single instillation. All developed microemulsions seem to outperform previously developed formulations for glaucoma treatment. Nevertheless, further efficacy and kinetic studies are needed to confirm the benefits of this novel therapeutic tool.

Declaration of competing interest

The authors declare no conflict of interest in any subjects treated in the present work.

Acknowledgements

Research Group UCM920415 (InnOftal), FEDER- CICYT (FIS-PI17/00079 and PI17/00466) and ISCIII-FEDER RETICS (OFTARED) (RD16/0008/0009 and RD16/0008/0004) that funded the present research work. We also acknowledge the access to cryoEM CNB-CSIC facility in the context of the CRIOMECORR project (ESFRI-2019-01-CSIC-16), and in to Rocío Arranz, Noelia Zamarreño y M. Teresa Bueno-Carrasco. All the figures were created with BioRender (www.biorender.com). M.G. C. thanks for a PhD fellowship from the Spanish MECD (FPU18/03445).

References

[1] Bourne RRA, Steinmetz JD, Saylan M, Mersha AM, Weldemariam AH, Wondmeneh TG, Sreeramareddy CT, Pinheiro M, Yaseri M, Yu C, Zastrozhin MS, Zastrozhina A, Zhang ZJ, Zimsen SRM, Yonemoto N, Tsegaye GW, Vu GT, Vongpradith A, Renzaho AMN, Sorrie MB, Shaheen AA, Shiferaw WS, Skryabin VY, Skryabina AA, Saya GK, Rahimi-Movaghar V, Shigematsu M, Sahraian MA, Naderifar H, Sabour S, Rathi P, Sathian B, Miller TR, Rezapour A, Rawal L, Pham HQ, Parekh U, Podder V, Onwujekwe OE, Pasovic M, Otstavnov N, Negash H, Pawar S, Naimzada MD, Al Montasir A, Ogbo FA, Owolabi MO, Pakshir K, Mohammad Y, Moni MA, Nunez-Samudio V, Mulaw GF, Naveed M, Maleki S, Michalek IM, Misra S, Swamy SN, Mohammed JA, Flaxman S, Park EC, Briant PS, Meles GG, Hayat K, Landires I, Kim GR, Liu X, LeGrand KE, Taylor HR, Kunjathur SM, Khoja TAM, Bicer BK, Khalilov R, Hashi A, Kayode GA, Carneiro VLA, Kavetskyy T, Kosen S, Kulkarni V, Holla R, Kalhor R, Jayaram S, Islam SMS, Gilani SA, Eskandarieh S, Molla MD, Itumalla R, Farzadfar F, Congdon NG, Elhabashy HR, Elayedath R, Couto RAS, Dervenis N, Cromwell EA, Dahlawi SMA, Resnikoff S, Casson RJ, Abdoli A, Choi JYJ, Dos Santos FLC, Abrha WA, Nagaraja SB, Abualhasan A, Adal TG, Aregawi BB, Beheshti M, Abu-Gharbieh E, Afshin A, Ahmadieh H, Alemzadeh SA, Arrigo A, Atnafu DD, Ashbaugh C, Ashrafi E, Alemayehu W, Alfaar AS, Alipour V, Anbesu EW, Androudi S, Arabloo J, Arditi A, Bagli E, Baig AA, Bärnighausen TW, Parodi MB, Bhagavathula AS, Bhardwaj N, Bhardwaj P, Bhattacharyya K, Bijani A, Bikbov M, Bottone M, Braithwaite T, Bron AM, Butt ZA, Cheng CY, Chu DT, Cicinelli MV, Coelho JM, Dai X, Dana R, Dandona L, Dandona R, Del Monte MA, Deva JP, Diaz D, Djalalinia S, Dreer LE, Ehrlich JR, Ellwein LB, Emamian MH, Fernandes AG, Fischer F, Friedman DS, Furtado JM, Gaidhane S, Gazzard G, Gebremichael B, George R, Ghashghaee A, Golechha M, Hamidi S, Hammond BR, Hartnett MER, Hartono RK, Hay SI, Heidari G, Ho HC, Househ M, Ibitoye SE, Ilic IM, Huang JJ, Ilic MD, Ingram AD, Irvani SSN, Jha RP, Kahloun R, Kandel H, Kasa AS, Kempen JH, Khairallah M, Khan EA, Khanna RC, Khatib MN, Kim JE, Kim YJ, Kisa A, Kisa S, Koyanagi A, Kurmi OP, Lansingh VC, Leasher JL, Leveziel N, Limburg H, Manafi N, Mansouri K, McAlinden C, Mohammadi SF, Mokdad AH, Morse AR, Naderi M, Naidoo KS, Nangia V, Nguyen HLT, Ogundimu K, Olagunju AT, Panda-Jonas S, Pesudovs K, Peto T, Ur Rahman MH, Ramulu PY, Rawaf DL, Rawaf S, Reinig N, Robin AL, Rossetti L, Safi S, Sahebkar A, Samy AM, Serle JB, Shaikh MA, Shen TT, Shibuya K, Il Shin J, Silva JC, Silvester A, Singh JA, Singhal D, Sitorus RS, Skiadaresi E, Soheili A, Sousa RARC, Stambolian D, Tadesse EG, Tahhan N, Tareque MI, Topouzis F, Tran BX, Tsilimbaris MK, Varma R, Virgili G, Wang N, Wang YX, West SK, Wong TY, Jonas JB, Vos T. Causes of blindness and vision impairment in 2020 and trends over 30 years, and prevalence of avoidable blindness in relation to VISION 2020: the Right to Sight: an analysis for the Global Burden of Disease Study. Lancet Global Health 2021;9:e144–60. https://doi.org/10.1016/S2214-109X(20)30489-7.

[2] Flaxman SR, Bourne RRA, Resnikoff S, Ackland P, Braithwaite T, Cicinelli MV, Das A, Jonas JB, Keeffe J, Kempen J, Leasher J, Limburg H, Naidoo K, Pesudovs K, Silvester A, Stevens GA, Tahhan N, Wong T, Taylor H, Arditi A, Barkana Y, Bozkurt B, Bron A, Budenz D, Cai F, Casson R, Chakravarthy U, Choi J, Congdon N, Dana R, Dandona R, Dandona L, Dekaris I, Del Monte M, Deva J, Dreer L, Ellwein L, Frazier M, Frick K, Friedman D, Furtado J, Gao H, Gazzard G, George R, Gichuhi S, Gonzalez V, Hammond B, Hartnett ME, He M, Hejtmancik J, Hirai F, Huang J, Ingram A, Javitt J, Joslin C, Khairallah M, Khanna R, Kim J, Lambrou G, Lansingh VC, Lanzetta P, Lim J, Mansouri K, Mathew A, Morse A, Munoz B, Musch D, Nangia V, Palaiou M, Parodi MB, Pena FY, Peto T, Quigley H, Raju M, Ramulu P, Reza D, Robin A, Rossetti L, Saaddine J, Sandar M, Serle J, Shen T, Shetty R, Sieving P, Silva JC, Sitorus RS, Stambolian D, Tejedor J, Tielsch J, Tsilimbaris M, van Meurs J, Varma R, Virgili G, Wang YX, Wang NL, West S, Wiedemann P, Wormald R, Zheng Y. Global causes of blindness and distance vision impairment 1990–2020: a systematic review and meta-analysis. Lancet Global Health 2017;5:e1221–34. https://doi.org/10.1016/S2214-109X(17)30393-5.

[3] Li T, Lindsley K, Rouse B, Hong H, Shi Q, Friedman DS, Wormald R, Dickersin K. Comparative effectiveness of first-line medications for primary open angle glaucoma – a systematic review and network meta-analysis. Ophthalmology 2016; 123:129–40. https://doi.org/10.1016/j.ophtha.2015.09.005.Comparative.

[4] Sambhara D, Aref AA. Glaucoma management: relative value and place in therapy of available drug treatments, Ther. Adv. Chronic Dis 2014;5:30–43. https://doi.org/10.1177/2040622313511286.

[5] Bazzaz S, Myers JS, Katz lJ. Latanoprost in the treatment of glaucoma. Clin Ophthalmol 2014;8:1967–85. https://doi.org/10.2147/OPTH.S59162.

[6] Gaudana R, Ananthula HK, Parenky A, Mitra AK. Ocular drug delivery. AAPS J 2010;12:348–60. https://doi.org/10.1208/s12248-010-9183-3.

[7] Noecker RJ. The management of glaucoma and intraocular hypertension: current approaches and recent advances. Therapeut Clin Risk Manag 2006;2:193–206. https://doi.org/10.2147/tcrm.2006.2.2.193.

[8] Sahoo SK, Dilnawaz F, Krishnakumar S. Nanotechnology in ocular drug delivery. Drug Discov Today 2008;13:144–51. https://doi.org/10.1016/j.drudis.2007.10.021.

[9] López-cano JJ, González-cela-casamayor MA, Herrero-vanrell R, Molina-martínez IT, Javier J, González-cela-casamayor MA, Herrero-vanrell R, Teresa I, Liposomes M. Liposomes as vehicles for topical ophthalmic drug delivery and ocular surface protection. Expet Opin Drug Deliv 2021;18:819–47. https://doi.org/10.1080/17425247.2021.1872542.

[10] Tsukamoto T, Hironaka K, Fujisawa T, Yamaguchi D, Tahara K, Tozuka Y, Takeuchi H. Preparation of bromfenac-loaded liposomes modified with chitosan for ophthalmic drug delivery and evaluation of physicochemical properties and drug release profile. Asian J Pharm Sci 2013;8:104–9. https://doi.org/10.1016/j.ajps.2013.07.013.

[11] Aggarwal D, Garg A, Kaur IP. Development of a topical niosomal preparation of acetazolamide: preparation and evaluation. J Pharm Pharmacol 2004;56:1509–17. https://doi.org/10.1211/0022357044896.

[12] Lancina III MG, Yang H. Dendrimers for ocular drug delivery. Can J Chem 2017;95: 897–902. https://doi.org/10.1139/cjc-2017-0193.

[13] Loftsson T, Stefánsson E. Cyclodextrins and topical drug delivery to the anterior and posterior segments of the eye. Int J Pharm 2017;531:413–23. https://doi.org/10.1016/j.ijpharm.2017.04.010.

[14] Yavuz B, Bozdağ Pehlivan S, Ünlü N. An overview on dry eye treatment: approaches for cyclosporin A delivery. Sci World J 2012. https://doi.org/10.1100/2012/194848. 2012.

[15] Wang H, Zhu Z, Zhang G, Lin F, Liu Y, Zhang Y, Feng J, Chen W, Meng Q, Chen L. AS1411 aptamer/hyaluronic acid-bifunctionalized microemulsion Co-loading shikonin and docetaxel for enhanced antiglioma therapy. J Pharmaceut Sci 2019; 108:3684–94. https://doi.org/10.1016/j.xphs.2019.08.017.

[16] Kotta S, Khan AW, Ansari SH, Sharma RK, Ali J. Formulation of nanoemulsion: a comparison between phase inversion composition method and high-pressure homogenization method. Drug Deliv 2015;22:455–66. https://doi.org/10.3109/10717544.2013.866992.

[17] Dhahir RK, Al-Nima AM, Al-Bazzaz FY. Nanoemulsions as ophthalmic drug delivery systems. Turkish J Pharm Sci 2021;18:652–64. https://doi.org/10.4274/tjps.galenos.2020.59319.

[18] Lallemand F, Daull P, Benita S, Buggage R, Garrigue J-S. Successfully improving ocular drug delivery using the cationic nanoemulsion. Novasorb, J Drug Deliv 2012:1–16. https://doi.org/10.1155/2012/604204. 2012.

[19] Vandamme TF. Microemulsions as ocular drug delivery systems: recent developments and future challenges. Prog Retin Eye Res 2002;21:15–34. https://doi.org/10.1016/S1350-9462(01)00017-9.

[20] Tartaro G, Mateos H, Schirone D, Angelico R, Palazzo G. Microemulsion microstructure(s): a tutorial review. Nanomaterials 2020;10:1–40. https://doi.org/10.3390/nano10091657.

[21] Hegde RR, Verma A, Ghosh A. Microemulsion: new insights into the ocular drug delivery. ISRN Pharm 2013:1–11. https://doi.org/10.1155/2013/826798. 2013.

[22] Rusciano D, Roszkowska AM, Gagliano C, Pezzino S. Free amino acids: an innovative treatment for ocular surface disease. Eur J Pharmacol 2016;787:9–19. https://doi.org/10.1016/j.ejphar.2016.04.029.

[23] Monaco G, Cacioppo V, Consonni D, Troiano P. Effects of osmoprotection on symptoms, ocular surface damage, and tear film modifications caused by glaucoma therapy. Eur J Ophthalmol 2011;21:243–50. https://doi.org/10.5301/EJO.2010.5730.

[24] Corrales RM, Luo L, Chang EY, Pflugfelder SC. Effects of osmoprotectants on hyperosmolar stress in cultured human corneal epithelial cells. Cornea 2008;27: 574–9. https://doi.org/10.1097/ICO.0b013e318165b19e.

[25] Fini ME, Bauskar A, Jeong S, Wilson MR. Clusterin in the eye: an old dog with new tricks at the ocular surface. Exp Eye Res 2016;147:57–71. https://doi.org/10.1016/j.exer.2016.04.019.

[26] Matysik-Woźniak A, Paduch R, Maciejewski R, Jünemann AG, Rejdak R. The impact of oleanolic and ursolic acid on corneal epithelial cells in vitro. Ophthalmol Times J 2017;1:124–32. https://doi.org/10.5603/oj.2016.0024.

[27] Ivanova S, Tonchev V, Yokoi N, Yappert MC, Borchman D, Georgiev GA. Surface properties of squalene/meibum films and NMR confirmation of squalene in tears. Int J Mol Sci 2015;16:21813–31. https://doi.org/10.3390/ijms160921813.

[28] Lee BM, Park SJ, Noh I, Kim CH. The effects of the molecular weights of hyaluronic acid on the immune responses. Biomater Res 2021;25:1–13. https://doi.org/10.1186/s40824-021-00228-4.

[29] Sanchez MA, Torralbo-jimenez P, Giron N, De Heras B, Vanrell RH, Arriola-villalobos P, Diaz-valle D, Alvarez-barrientos A. Comparative analysis of carmellose 0.5% versus hyaluronate 0.15% in dry eye: a flow cytometric study. Cornea 2010;29:167–71.

[30] López-Cano JJ, González-Cela-Casamayor MA, Andrés-Guerrero V, Herrero-Vanrell R, Benítez-Del-Castillo JM, Molina-Martínez IT. Combined hyperosmolarity and inflammatory conditions in stressed human corneal epithelial cells and macrophages to evaluate osmoprotective agents as potential DED treatments. Exp Eye Res 2021;211:108723. https://doi.org/10.1016/j.exer.2021.108723.

[31] Gómez-Ballesteros M, López-Cano JJ, Bravo-Osuna I, Herrero-Vanrell R, Molina-Martínez IT, Gómez-Ballesteros M, López-Cano JJ, Bravo-Osuna I, Herrero-Vanrell R, Molina-Martínez IT. Osmoprotectants in hybrid liposome/HPMC systems as potential glaucoma treatment. Polymers 2019;11:929. https://doi.org/10.3390/polym11060929.

[32] Lopez-Cano JJ, González-cela-casamayor MA, Andrés-Guerrero V, Vicario-de-la-Torre M, Benitez-del-castillo JM, Vanrell RH, Molina-Martínez IT. Development of an osmoprotective microemulsion as a therapeutic platform for ocular surface protection. Int J Pharm 2022;623:1–13. https://doi.org/10.1016/j.ijpharm.2022.121948.

[33] Masaki Y, Tanaka M, Nishikawa T. Physicochemical compatibility of propofol-lidocaine mixture. Anesth Analg 2003;97:1646–51. https://doi.org/10.1213/01.ANE.0000087802.50796.FB.

[34] Patel P, Priti P, Giram P. Bioanalytical method development and validation for latanoprost quantification in pharmaceutical opthalmic microemulsion formulation by RP-HPLC. UNIMAID J Priv Prop Law 2015;6. https://doi.org/10.4172/2155.

[35] Gagliano C, Papa V, Amato R, Malaguarnera G, Avitabile T. Measurement of the retention time of different ophthalmic formulations with ultrahigh-resolution optical coherence tomography. Curr Eye Res 2018;43:499–502. https://doi.org/10.1080/02713683.2017.1418893.

[36] Grassiri B, Zambito Y, Bernkop-Schnürch A. Strategies to prolong the residence time of drug delivery systems on ocular surface. Adv Colloid Interface Sci 2021; 288. https://doi.org/10.1016/j.cis.2020.102342.

[37] European Medicines Agency. Guideline on the investigation of bioequivalence discussion. 2010. https://doi.org/CPMP/EWP/QWP/1401/98 Rev. 1/ Corr **.

[38] Hotujac Grgurević M, Juretić M, Hafner A, Lovrić J, Pepić I. Tear fluid-eye drops compatibility assessment using surface tension. Drug Dev Ind Pharm 2017;43: 275–82. https://doi.org/10.1080/03639045.2016.1238924.

[39] Dutescu RM, Panfil C, Schrage N. Osmolarity of prevalent eye drops, side effects, and therapeutic approaches. Cornea 2015;34:560–6. https://doi.org/10.1097/ICO.0000000000000368.

[40] Rahić O, Tucak A, Omerović N, Sirbubalo M, Hindija L, Hadžiabdić J, Vranić E. Novel drug delivery systems fighting glaucoma: formulation obstacles and solutions. Pharmaceutics 2021;13:1–58. https://doi.org/10.3390/pharmaceutics13010028.

[41] Boso ALM, Gasperi E, Fernandes L, Costa VP, Alves M. Impact of ocular surface disease treatment in patients with glaucoma. Clin Ophthalmol 2020;14:103–11. https://doi.org/10.2147/OPTH.S229815.

[42] Jones L, Downie LE, Korb D, Benitez-del-Castillo JM, Dana R, Deng SX, Dong PN, Geerling G, Hida RY, Liu Y, Seo KY, Tauber J, Wakamatsu TH, Xu J, Wolffsohn JS, Craig JP. TFOS DEWS II management and therapy report. Ocul Surf 2017;15: 575–628. https://doi.org/10.1016/j.jtos.2017.05.006.

[43] Gautam N, Kesavan K. Phase transition microemulsion of brimonidine tartrate for glaucoma therapy: preparation, characterization and pharmacodynamic study. Curr Eye Res 2021;46:1844–52. https://doi.org/10.1080/02713683.2021.1942071.

[44] Xu W, Jiao W, Li S, Tao X, Mu G. Bimatoprost loaded microemulsion laden contact lens to treat glaucoma. J Drug Deliv Sci Technol 2019;54:101330. https://doi.org/10.1016/j.jddst.2019.101330.

[45] Sakai Y, Yasueda SI, Ohtori A. Stability of latanoprost in an ophthalmic lipid emulsion using polyvinyl alcohol. Int J Pharm 2005;305:176–9. https://doi.org/10.1016/j.ijpharm.2005.08.017.

[46] Labetoulle M, Benitez-del-castillo JM, Barabino S, Vanrell RH, Daull P, Garrigue J, Rolando M. Artificial tears : biological role of their ingredients in the management of dry eye disease, vol. 23; 2022.

[47] Shen LN, Zhang YT, Wang Q, Xu L, Feng NP. Preparation and evaluation of microemulsion-based transdermal delivery of total flavone of rhizoma arisaematis. Int J Nanomed 2014;9:3453–64. https://doi.org/10.2147/IJN.S66524.

[48] Mathews RG, Donald AM. Conditions for imaging emulsions in the environmental scanning electron microscope. Scanning 2002;24:75–85. https://doi.org/10.1002/sca.4950240205.

[49] Cizmar P, Yuana Y. Detection and characterization of extracellular vesicles by transmission and cryo-transmission electron microscopy. In: Patrick Kuo W, Jia S,

editors. Extracell. Vesicles methods protoc. Methods mol. Biol.; 2017. p. 221–32. https://doi.org/10.1525/9780520948068-021.
[50] Lawton JR. An investigation of the fixation and staining of lipids by a combination of malachite green or other triphenylmethane dyes with glutaraldehyde. J Microsc 1988;154:83–92. https://doi.org/10.1111/j.1365-2818.1989.tb00570.x.
[51] Ismail A, Nasr M, Sammour O. Nanoemulsion as a feasible and biocompatible carrier for ocular delivery of travoprost: improved pharmacokinetic/pharmacodynamic properties. Int J Pharm 2020;583:119402. https://doi.org/10.1016/j.ijpharm.2020.119402.
[52] Smedowski A, Paterno JJ, Toropainen E, Sinha D, Wylegala E, Kaarniranta K. Excipients of preservative-free latanoprost induced inflammatory response and cytotoxicity in immortalized human HCE-2 corneal epithelial cells. J Biochem Pharmacol Res 2014;2:175–84. http://www.ncbi.nlm.nih.gov/pubmed/25530926%0Ahttp://www.pubmedcentral.nih.gov/articlerender.fcgi?artid=PMC4270205.
[53] Trzeciecka A, Paterno JJ, Toropainen E, Koskela A, Podracka L, Korhonen E, Kauppinen A, Kaarniranta K, Smedowski A. Long-term topical application of preservative-free prostaglandin analogues evokes macrophage infiltration in the ocular adnexa. Eur J Pharmacol 2016;788:12–20. https://doi.org/10.1016/j.ejphar.2016.06.014.
[54] Soriano-Romaní L, Vicario-de-la-Torre M, Crespo-Moral M, López-García A, Herrero-Vanrell R, Molina-Martínez IT, Diebold Y. Novel anti-inflammatory liposomal formulation for the pre-ocular tear film: in vitro and ex vivo functionality studies in corneal epithelial cells. Exp Eye Res 2017;154:79–87. https://doi.org/10.1016/j.exer.2016.11.010.
[55] Goldstein A, Soroka Y, Frušić-Zlotkin M, Popov I, Kohen R. High resolution SEM imaging of gold nanoparticles in cells and tissues. J Microsc 2014;256:237–47. https://doi.org/10.1111/jmi.12179.
[56] Zheng Y, Xu G, Ni Q, Wang Y, Gao Q, Zhang Y. Microemulsion delivery system improves cellular uptake of genipin and its protective effect against A β 1-42-induced PC12 cell cytotoxicity. 2022. p. 1–21.
[57] Carmona-Ule N, Abuín-Redondo C, Costa C, Piñeiro R, Pereira-Veiga T, Martínez-Pena I, Hurtado P, López-López R, de la Fuente M, Dávila-Ibáñez AB. Nanoemulsions to support ex vivo cell culture of breast cancer circulating tumor cells. Mater Today Chem 2020;16. https://doi.org/10.1016/j.mtchem.2020.100265.
[58] Bellenger-Germain S, Poisson JP, Narce M. Antihypertensive effects of a dietary unsaturated FA mixture in spontaneously hypertensive rats. Lipids 2002;37:561–7. https://doi.org/10.1007/s11745-002-0933-z.
[59] Nowacki D, Martynowicz H, Skoczyńska A, Wojakowska A, Turczyn B, Bobak Ł, Trziszka T, Szuba A. Lecithin derived from ω-3 PUFA fortified eggs decreases blood pressure in spontaneously hypertensive rats. Sci Rep 2017;7:1–11. https://doi.org/10.1038/s41598-017-12019-w.
[60] Yarishkin O, Phuong TTT, Bretz CA, Olsen KW, Baumann JM, Lakk M, Crandall A, Heurteaux C, Hartnett ME, Križaj D. TREK-1 channels regulate pressure sensitivity and calcium signaling in trabecular meshwork cells. J Gen Physiol 2018;150:1660–75. https://doi.org/10.1085/jgp.201812179.
[61] De Kater AW, Spurr-Michaud SJ, Gipson IK. Localization of smooth muscle myosin-containing cells in the aqueous outflow pathway. Investig Ophthalmol Vis Sci 1990;31:347–53.
[62] Cuppoletti J, Malinowska DH, Tewari KP, Chakrabarti J, Ueno R. Unoprostone isopropyl and metabolite M1 activate BK channels and prevent ET-1-induced [Ca2+]i increases in human trabecular meshwork and smooth muscle. Investig Ophthalmol Vis Sci 2012;53:5178–89. https://doi.org/10.1167/iovs.11-9046.
[63] Daull P, Buggage R, Lambert G, Faure MO, Serle J, Wang RF, Garrigue JS. A comparative study of a preservative-free latanoprost cationic emulsion (catioprost) and a BAK-preserved latanoprost solution in animal models. J Ocul Pharmacol Therapeut 2012;28:515–23. https://doi.org/10.1089/jop.2011.0245.